University of Stavanger

Faculty of Science and Technology

MASTER'S THESIS

Study program/ Specialization: Petroleum technology Drilling Technology	Spring semester, 2011 Restricted
Writer: Farzad Basardeh	…… (Writer's signature)
Faculty supervisor: Dr. Mesfin Belayneh External supervisor(s): Dr. Gunnstein Sælevik	
Title/working title of thesis: *Monitoring of real time drilling opretional processes, and early downhole problems detection*	
Credits (ECTS): 30	
Key words: DrillSceen, Real-time,	Pages: ……80…… + enclosure: …..…… Stavanger, …15/2012…….. Date/year

Preface

This master thesis has been carried out at the Department of the Petroleum Engineering, University of Stavanger, Norway, under the supervision of Associate Professor Mesfin Belayneh during the spring term 2012.

I wish to express my deep gratitude to Mesfin Belayneh for supervising me during this work and providing with generous ideas and constructive comments during my work. Our discussions and your feedback have been very inspiring and useful. I would like to thank Sekal AS Norway for providing data and DrillScene. In particular I would like to appreciate Gunnstein Sælevik Project manager in the onshore drilling center in Sekal AS, his necessary support and guidance.

Finally, I thank my family for providing me the unconditional support necessary to finish this thesis and during my education in general.

Farzad Basardeh

June 15, 2012

Abstract

In this thesis work, the real-time drilling monitoring software, DrillScene^{TM} has been used to monitor two case studies of wellbores drilled in North-Sea, Norway. Basically the thesis consists of three main parts:

- DrillScene is based on advanced models. Because of confidentiality, it is not possible to review the models. Therefore, for better understanding of drilling response, the first part reviews simple basic models. These are mechanical, hydraulic, thermodynamic and cutting transport models.

- The second part is to review research papers related to DrillScene monitoring of downhole conditions. This part describes how the system set up and data acquisition of the software work, calculations processes and how the models simultaneously calibrated as it goes along with monitoring.

- Finally, using DrillScene to monitor drilling operations of two wells drilled in Norwegian Continental Shelf (NCS). The monitoring was carried out at SEKAL AS onshore drilling operation center. The results of monitoring have been comprehensively explained. These results contain how DrillScene can be used to detect any drilling problem ahead of the dangerous situation in order to avoid it as well as giving advice of how the ongoing operation could be optimized.

List of figures

List of Tables

List of symbols

T = torque

θ = inclination

α = Azimuth

wi =weight per unit length

β = Buoyance factor

ρ_{o1}, ρ_{w1}= density of oil and water at temperature T_1 and pressure P_1, respectively

ρ_{o2}, ρ_{w2}= density of oil and water at temperature T_2 and pressure P_2, respectively

f_{vo}, f_{vw}, f_{vs}, f_{vc} = fractional volume of oil, water, solid weighting material, and chemical additives, respectively

ρ_{ecd}= equivalent circulating density (lb/gal)

$\Delta P_{hydrostatic}$ = Hydrostatic head of fluid column (psi)

$\Delta P_{friction}$ = Pressure drop due to friction in the annulus (psi)

D_{hy} = the hydraulic diameter

D_{hy} = D for drill-string

$D_{hy} = D_o - D_f$ for annulus

v_{mix} = the fluid mixture velocity

D_e= equivalent diameter

A_f = cross-sectional area

P_w = wetted perimeter

N= generalization power law index

ε = wall roughness

Pt = Standpipe pressure, psi

Pcs = Pressure loss in surface connection, spsi

Pdb = Pressure loss through drill pipe, psi

Pdc = Pressure loss through drill collars, psi

Pb = pressure loss through bit nozzles, psi

Pdca = pressure loss through hole-drill collar annulus, psi

Pdpa = pressure loss through hole-drill pipe annulus, psi

D_{eff} = effective diameter

F_i =bottom weight

List of abbreviation

BHA =Bottom Hole Assembly

ECD = Equivalent Circulation Density

ESD = Equivalent Static Density

FIT = Formation Integrity Test

HTTP = Hyper Text Transfer Protocol

HWDP =Heavy Weight Drill Pipe

IRIS = International Research Institute of Stavanger

LCM = Lost Circulation Material

LWD = Logging while Drilling

MD = Measured Depth

MPD = Managed Pressure Drilling

MWD = Measurement While Drilling

POOH = Pull Out Of Hole

PP = Pore Pressure

PVT = Pressure Volume Temperature

RIH = Run In Hole

ROP = Rate of Penetration

RPM = Revolution per Minute

SQL = Structured Query Language

TCP = Transmission Control Protocol

TD = Target Depth

FRW = Free Rotating Weight Deviations

Table of Contents

1. Introduction

1.1 Background of the thesis

Figure 1shows the well program to avoid, wellbore instability such as well collapse and fracturing. The design is based on formation pressure, in-situ stresses and rock mass strength. . In average the wellbore instability problems alone increase 10-15% of the overall drilling budget [1].

If the well pressure is lower than the formation pressure or close, formation fluids may influx to the well. This results in a kick. At a worst case scenario, if out of control, the kick may leads to Blow-out conditions. In addition, low well bore pressure can also lead to formation instability, causing the walls of the well bore to collapse. The fragments as a result lead to pack-off and bridging, which hinders fluid circulation and drill string movement.

The density of the mud is usually kept high enough so that hydrostatic pressure in the mud column is greater than formation pressure. This pressure difference forces some of the drilling fluid to invade porous and permeable formations. As invasion occurs, many of the solid particles (i.e., clay minerals from the drilling mud) are trapped on the side of the borehole and form mud cake. Fluid that filters into the formation during invasion is called mud filtrate. As a result filtrate causes formation damage, and good mud cake also has on well strengthening effect.

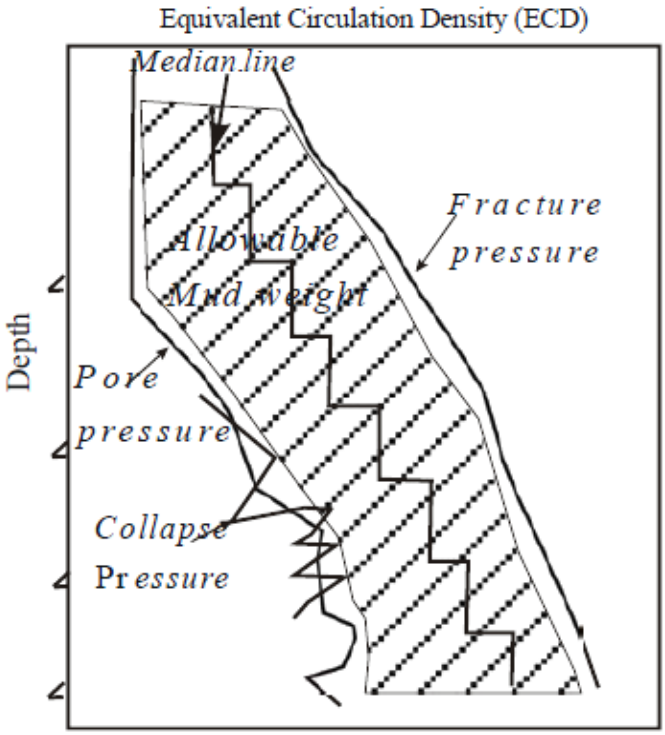

Figure 1: Depth versus Equivalent Circulation Density (ECD) [2]

Downhole conditions can become worse during drilling operation and this lead to unexpected situation which can result unnecessary delays.

In traditional drilling, the cost of drilling operation increases as a result of the non-productive time due to unplanned well incident. The main problems that occur during drilling operation are, such as kick, stuck pipe, wellbore collapse, lost circulation and equipment failures.

Table 1 below shows an example that give an overview over the time consuming related to bore-hole stability. As the table shows if the average time to drill is 60 days, unexpected borehole stability problems account around 15% of the time consuming [2]. So borehole stability is going to become a more important issue during drilling operations.

Event	**Time used (days):**
Circulation losses	15
Tight hole	2
Squeeze cementing	15
Stuck casing	20
Fishing	2
Total	52 days
Per well	52/6=8.7 days

Table 1: Time consumption related to borehole stability [2].

To reduce this non-productive time one need to apply a methodology which could discover deterioration of downhole condition during drilling and then takes pre-emptive action to avoid any drilling incident that can be occur. It needs a system which is based on application of advanced real-time process models for calculation of the various physical forces acting inside the well (mechanical, hydraulic and thermodynamic). These physical forces are connected by an automatic model calibration; by analyzing of the deviation between modeled and measured values one can estimate the current situation of the well with real time data and then warn the drilling team of deterioration of the downhole condition.

During the last decade, many companies tried to analyses well operation problems by computer. International Research Institute of Stavanger (IRIS) has developed advanced computer models for monitoring the drilling operation, called DrillScene^{TM}. This thesis work is based on the DrillScene^{TM} technology and will focus on analyzing in detail how this automated system used in drilling operations to detect drilling incidence.

1.2 Scope and objective of the thesis

The scope of the thesis is based on literature study and interpretation of the downhole condition using DrillScene ^{TM} package.

The main objective of the thesis is to perform monitoring and detection of down hole condition. The main activities are:

- Literature study on the basics of the mechanical, hydraulic and cutting transport models in order to understand processes in drilling well

- To review the research results performed by IRIS regarding interpretation of the monitoring and detection of down hole condition. In addition to review the general structure of the DrillScene architecture.

- Finally, to perform monitoring and detection of cases wells operated in North Sea area section by section. This is performed by monitoring different operational parameters and comparing different symptoms for any challenges that might come up in the wellbore. Because of confidentiality some of the information regarding the area, depth and other sensitive information will be restricted

2. DrillScene Models

DrillScene is built based on advanced models. Because of conditionality, it is difficult to get access for these models. DrillScene technology takes and calculates all of the physical parameters of a drilling operation. From the DrillScene manual and monitoring display, it is observed that DrillScene is based on the mechanical, hydraulic, thermodynamic and cutting transport models. These models are connected together. In this chapter, basic models will be reviewed in order to understand the interpretation of the responses in real time data.

2.1 Mechanical model

Torque and drag problems are very common during drilling, completion, and work over operations. Both torque and drag are assumed to be caused by sliding friction force that can be result from contact with the drill string with the wellbore. The sliding friction force is a function of the normal contact force and the coefficient of friction between the contact surfaces. The sliding friction is the proportion of the friction force to the normal force and this value depends on materials contact and the degree of lubrication at different places in the wellbore.

2.1.1 Drag

Drag is the force difference between free rotating weight and the force required to move the pipe up or down in the hole. Pick-up drag force is usually higher than static weight. While slack-off drag force is usually lower than static weight [3].

The most common assumption for Toque and drag modeling are:

- ***Slack string:*** This assumes that the drill string is continuously in contact with wellbore.
- ***Coulomb friction:*** The friction force on a drill string is due to the wellbore
- ***Soft string:*** contact force is due to the normal component of the weight of the drill string.
- ***Fluid flow effect:*** hydrodynamic force due to fluid flow has an effect on the drag force

The normal contact force between the pipe and well depends on the effect of gravity on the pipe and the effect of tension acting in the wellbore. These forces are shown in Figure 2.

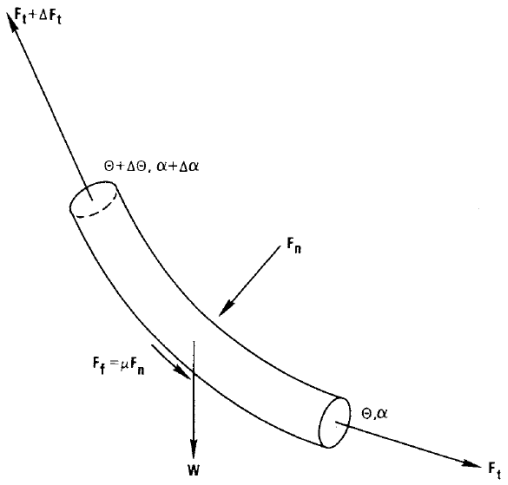

Figure 2: Force balance on drilling element illustrating sources of normal force [3]

Figure 2 shows the force acting on a short slightly curved element. F_n is the net normal force and negative vector sum of the normal components of the weight, W and from the two tension force, Ft and $F_t+\Delta F_t$. The friction calculation needs only the dimensions of the normal force, not its direction [3].

In any curved well geometry that shows variation in inclination and azimuth, the normal force per unit length has been derived by [**Error! Reference source not found.**]:

$$N_i = \sqrt{\left(\beta w_i \sin\left(\frac{\theta_{i+1}+\theta_i}{2}\right)+F_i\left(\frac{\theta_{i+1}-\theta_i}{S_{i+1}-S_i}\right)\right)^2+\left(F_i \sin\left(\frac{\theta_{i+1}+\theta_i}{2}\right)\left(\frac{\alpha_{i+1}-\alpha_i}{S_{i+1}-S_i}\right)\right)^2} \quad (2.1)$$

Where:

- θ = inclination
- α = Azimuth
- w_i =weight per unit length
- β = Buoyance factor

The contact force give in Eq. 2.1 used to derive drag force as:

$$F_{i+1} = F_i + \sum_{i=1}^{n}\left[\beta w_i \cos\left(\frac{\theta_{i+1}+\theta_i}{2}\right) \pm \mu_{ai} N_i\right](S_{i+1}-S_i) \quad (2.2)$$

Where the plus and minus sign allows for pipe movement direction whether running in or pulling out of the hole. The plus sign is for upward motion where friction adds to the axial load and the minus sign is for downward motion where the opposite is the case.F_i is the bottom weight when integrating from the bottom to top type.

2.1.2 Torque

Generally torque or moment is a result of force multiplied with by an arm. In drilling, torque is the moment required to rotate the pipe. The moment should be used to overcome the rotational friction in the well and on the bit with the formation. High drag forces and high torque are normally associated with each other. In an ideal vertical well the torque loss would be zero, except for a small loss due to viscous force resulted by mud. In a deviated well the torque loss may be significant, especially in long complex or extended reach well. In this condition torque loss is a major limiting factor to how long drilling can be continued. Torque is dependent to the radius of which rotation occurs and the friction coefficient and the normal force over pipe [5].
The increment torque calculation is:

$$\Delta T = \mu N_i r \Delta S \tag{2.3}$$

For both buckled and non-buckled string the torque loss per unit length is expressed as

$$T_{i+1} = T_i + \sum_{i=1}^{n} \mu . r_i . N_i . (S_{i+1} - S_i) \tag{2.4}$$

Buoyancy factor

The presence of fluid in the well and pipe has effect on the torque and drag models. The buoyancy factor, which modifies the weight of drill string, is given as [6]:

$$\beta = 1 - \frac{\rho_o A_o - \rho_i A_i}{\rho_{pipe}(A_o - A_i)} \tag{2.5}$$

Where, the subscript “o” and “i” are the outer and the inside of the drill string. A_i and A_o are the outer and inner area of drill string. If the inside (A_i) and the outside (A_o) drilling fluid densities are equal, Eq. (2.5) will be reduced to Eq. (2.6) as:

$$\beta = 1 - \frac{\rho_{mud}}{\rho_{pipe}} \tag{2.6}$$

A heavy mud will decrease the effective weight of the drill string, so this can decrease the side force and the loads from friction and torque. However a heavy mud has higher friction due to weighing particles and less lubricant.

2.2 Hydraulics models

2.2.1 Rheology models

Rheology can be defined as the knowledge and study of deformation and flow; it refers to the different properties and characteristics of drilling fluid. The major application of rheological properties for evaluating drilling behavior are in solving problems of hole cleaning and hole erosion of cuttings, hydraulic calculations, and drilling fluid treatment [7].

Rheological models try to obtain to characterize flow behaviors by developing relationships between applied shear stress, and the shear rate of the fluid. Based on the nature of this relationship, fluids in general can be classified as Newtonian, non-Newtonian, and viscoelastic fluids. Table 2 shows an example of rheology measured data.

Reading	Value
$\mathbf{R_{600}}$	92
$\mathbf{R_{300}}$	58
$\mathbf{R_{200}}$	46
$\mathbf{R_{100}}$	32
$\mathbf{R_{6}}$	10
$\mathbf{R_{3}}$	8

Table 2: Rheology measured data.

2.2.1.1 Bingham Plastic Model

The Bingham plastic model is the first two-parameter model. The fluid is represented as a newton fluid it mean time-independent and is shown by linear relationship between the applied stress and the rate of shear. However, it does not represent accurately the behavior of the drilling fluid at very low shear rates (in the annulus) or at very high shear rate (at the bit). The equation for Bingham plastic model is given as [8]:

$$\tau = \tau_y + \mu_p \gamma \qquad (\tau > \tau_y) \qquad (2.7)$$

The Bingham parameters, yield point (τ_y) and plastic viscosity (μ_p) can be read from a graph or can be calculated by the following equations,

$$\mu_p = R_{600} - R_{300} \qquad (2.8)$$

$$\tau_y = R_{300} - \mu_p \qquad (2.9)$$

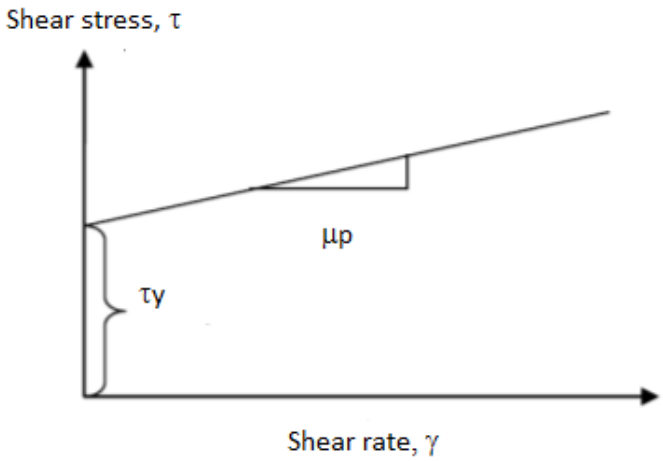

Figure 3: Bingham Plastic Model [18].

2.2.1.2 Power Law Model

The Bingham plastic model assumes a linear relationship between shear stress and shear rate and also it is a time-independent two parameter rheological model [8]. However, a better representation of the behavior of a drilling fluid is to consider a Power-law relationship between viscosity and shear rate such that:

$$\tau = K\gamma^n \tag{2.10}$$

Where *k* is the consistence index and *n* is flow behavior index. K is a measure of the consistency of the fluid, the higher the value of k the more viscous the fluid, n is a measure of the degree of non-Newtonian behavior of the fluid. Parameter constraints are K>0 and 0<n<1.

Eq. 2.10 was linearized as follows:

$$\log \tau = \log k + n \log y \tag{2.11}$$

Where *n* is determined from the slope and *k* is the intercept.

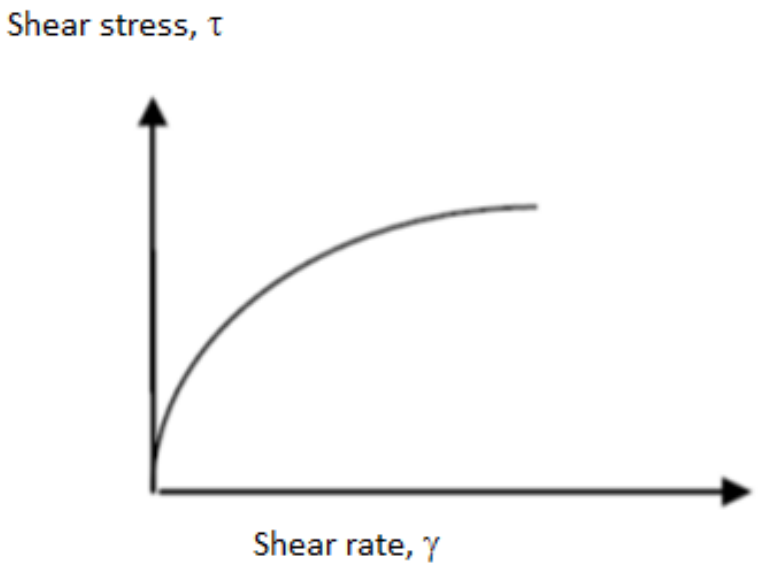

Figure 4: Power Law Model [18].

2.2.1.3 Robertson and Stiff Model

Robertson and Stiff developed a three-parameter model and more general model to describe the rheological behavior of drilling fluids and cement slurries [8]. The basic equation is:

$$\tau = A(\gamma + C)^B \qquad (\tau > AC^B) \tag{2.12}$$

Where *A, B, and C* are model parameters. *A* and *B* can be considered similar to the parameters *k* and *n* of the Power-law model. The third parameter *C* is a correction factor to the shear rate, and the term $(\gamma + c)$ is considered effective shear rate.

Eq. 2.14 represents the yield stress for the Robertson and Stiff model.

$$\tau_o = AC^B \tag{2.13}$$

To evaluate the parameters, we plotted the shear stress corresponding to several shear rates. The logarithm from Eq. 2.13 plots a straight line on log-log coordinates:

$$\text{Log}(\tau) = \log(A) + B\log(\gamma + C) \tag{2.14}$$

Thus, if τ is plotted vs. $(\gamma + C)$ on log-log coordinates, *B* is the slope and *A* is the intercept where $(\gamma + C) = 1.0$.

$C = (\gamma_{min}\gamma_{max} - \gamma^{*2}) / (2\gamma^{*} - \gamma_{min} - \gamma_{max})$ (2.15)

Where γ^{*} is the shear rate value corresponding to the geometric mean of the shear stress, τ^{*}.

The geometric mean of the shear stress (τ^{*}) is then calculated from:

$\tau^{*} = (\tau_{min} \times \tau_{max})^{1/2}$. (2.16)

2.2.2 PVT models

There are two major methods of characterizing the variation of the downhole conditions in responds to change in temperature of drilling fluid:

1. Analytical models
2. Empirical models

2.2.2.1 Analytical models

Hoberock Compositional Model: Mud density changes at different downhole elevated due to the mud compress under pressure and expand with temperature. Study of the compositional model needs some knowledge of how the densities of each liquid phase in the mud change with changes in temperature and pressure. To plane well control, to prevent lost circulation and to analyze fracture gradient test data one should be able predict the mud density at elevated pressure and temperature by knowledge of composition.

Hoberock et al. presented a compositional material-balance for predicting downhole densities for water-and diesel oil based muds and the mud density at elevated pressure and temperature [9]. The following compositional model is:

$$\rho(p,T) = \frac{\rho_{o1} f_{vo} + \rho_{w1} f_{vw} + \rho_s f_{vs} + \rho_c f_{vc}}{1 + f_{vo}\left(\frac{\rho_{o1}}{\rho_{o2}} - 1\right) + f_{vw}\left(\frac{\rho_{w1}}{\rho_{w2}} - 1\right)} \quad (2.17)$$

Where:

ρ_{o1}, ρ_{w1}= density of oil and water at temperature T_1 and pressure P_1, respectively

ρ_{o2}, ρ_{w2}= density of oil and water at temperature T_2 and pressure P_2, respectively

f_{vo}, f_{vw}, f_{vs}, f_{vc} = fractional volume of oil, water, solid weighting material, and chemical additives, respectively

2.2.2.2 Empirical models

Glasø's correlation : Pressure –volume-temperature (PVT) correlation are important in reservoir technology, and uses for estimating the amount of oil in the reservoir, production capacity, and variations in producing gas/oil ratios during the reservoir's production life also are a necessity for calculating the recovery the productivity of a reservoir [10].

Sorelle correlation: A mathematical model to introduce an accurate and reliable method of predicting the influence of downhole conditions on the density of the drilling fluid column and the hydrostatic pressure of input data. It is a general model for oil and water base drilling fluids and completion fluids [11].

Standing correlation: This model presents correlation of bubble-point pressures, formation volumes of bubble-point liquids, and formation volumes of gas plus liquid phases as empirical functions of gas-oil ratio, gas gravity, oil gravity, pressure and temperature [12].

2.2.3 Equivalent Circulating density (ECD)

The equivalent circulating density of a drilling fluid can be defined as the sum of the hydrostatic head of the fluid column, and the pressure loss in the annulus due to fluid flow. It is expressed as density term at the point of interest [13].

$$\rho_{ecd} = \frac{\Delta P_{hydrostatic} + \Delta P_{friction}}{g \times h} \tag{2.18}$$

Where:

- ρ_{ecd}= equivalent circulating density (lb/gal)
- $\Delta P_{hydrostatic}$ = Hydrostatic head of fluid column (psi)
- $\Delta P_{friction}$ = Pressure drop due to friction in the annulus (psi)

The hydrostatic pressure of the drilling fluid is affected by the temperature-pressure conditions present in the well-bore, and the depth of the well-bore. The frictional pressure loss is affected by the well-bore and drill string geometry, fluid rheology, and the pump rate or fluid flow rate.

2.2.4 Friction Pressure Loss Model

The frictional pressure loss is the loss in pressure during fluid flow due to contact between the fluid and the walls of the flow channel. The viscous property of the fluid creates a variation in the flow velocity normal to the solid interface, ranging from zero at the pipe wall with a no-slip assumption and maximum velocity at the edge of the boundary layer. This variation in fluid velocity represents a loss in momentum and a resistance to flow [13]. The friction pressure loss for both drill-string and annulus flow is calculated using the relation [14]:

$$K = c.\frac{2f}{D_{hy}}\rho_{mix}.v_{mix}^2 \quad (2.19)$$

Where:

D_{hy} = the hydraulic diameter

D_{hy} = D for drill-string

$D_{hy} = D_o - D_f$ for annulus

v_{mix} = the fluid mixture velocity

The Fanning friction f is calculated according to the rheological model chosen, and the current flow regime. The coefficient c is a calibration factor that can be used to adjust the model to the measurements in real-time if a proper calibration technique is chosen. The initial value is 1. The friction factors can be used to adjust the flow model if a proper estimation algorithm is implemented. The factors will then be updated in real-time by chosen algorithm to obtain an optimal match between measured and calculated results [14].

In the case of non-circular flow conduits, the diameter parameter is replaced by the equivalent diameter.

$$D_e = 4\times\frac{A_f}{P_w} \quad (2.20)$$

Where:

D_e= equivalent diameter

A_f = cross-sectional area

P_w = wetted perimeter

In addition the wall roughness, pipe inclination and flow regime is important. In single phase and multiphase flow the discrimination between laminar and turbulent flow plays an important role in the friction pressure loss. The type of flow is determined from the Reynolds number:

$$N_{Re} = \frac{\rho v D_{eff}}{\mu_{app}} \quad (2.21)$$

In Eq.2.21, D_{eff} is the effective diameter that accounts for both geometry and the effects of non-Newtonian fluid. μ_{app} is the apparent viscosity.

The effective diameter for the drill-string is given by [15]:

$$D_{eff} = D\frac{4N}{3N+1} \quad (2.22)$$

And for the annulus:

$$D_{eff} = 2/3(D_o - D_i)\frac{3N}{2N+1} \quad (2.23)$$

Where:

N= generalization power law index

The discrimination between flow model regimes:

$N_{Re} \leq 2000$ Laminar flow

$2000 < N_{Re} \leq 4000$ Transition between laminar and turbulent flow

$4000 < N_{Re}$ Turbulent flow

The total pressure gradient in the pipe can be considered as composed of 3 different terms: potential energy change (which is the hydrostatic pressure component), kinetic energy change (which is accounted for by the acceleration term), and a third contribution due to the frictional pressure losses [15] [16].

$$\frac{dp}{dz} = \left(\frac{\partial p}{\partial p}\right)_{hydrostatic} + \left(\frac{\partial p}{\partial z}\right)_{acceleration} + \left(\frac{\partial p}{\partial z}\right)_{friction} \quad (2.24)$$

The individual terms are defined as below:

$$\left(\frac{\partial p}{\partial z}\right)_{hydrostatic} = g.\rho.sin\theta \quad (2.25)$$

$$\left(\frac{\partial p}{\partial z}\right)_{acceleration} = -\rho.v\frac{dv}{dL} \quad (2.26)$$

$$\left(\frac{\partial p}{\partial z}\right)_{friction} = \frac{f.\rho.v^2}{2d} \quad (2.27)$$

The contributions from each of these are different in single phase and two phase flow.
The coefficient f in laminar flow is given by the Reynolds number N_{Re} as:

$$f = \frac{16}{N_{Re}} \tag{2.28}$$

To find the turbulent friction the equation below is used:

$$\frac{1}{\sqrt{f}} = -4log_{10}\left[\frac{0.27\varepsilon}{D_{eff}} + 1.26^{N^{-12}}/(N_{Re}f^{1-\frac{N}{2}})^{N^{-0.75}}\right] \tag{2.29}$$

Where:
ε, is wall roughness.

2.2.5 Stand Pipe pressure (SPP)

Downhole static pressures are easy to calculate from mud weight measured at the surface, while additional pressures caused by circulation can be calculated using established relationships between the pump rate and drilling fluid rheological properties.

During circulating of drilling fluid, friction between the drilling fluid and the wall of the drill pipe and annulus cause pressure loss.

Actually, the pump pressure, Δp_p, is affected by [17]:

1. Frictional pressure losses (Δps) in the surface equipment such as Kelly, swivel, standpipe.
2. Frictional pressure losses (Δp_{ds}) inside the drill-string (drill-pipe, Δp_{dp} and drill collar, Δp_{dc}).
3. Frictional pressure losses across the bit, Δp_b.
4. Frictional pressure losses in the annulus around the drill-string, Δp_a.

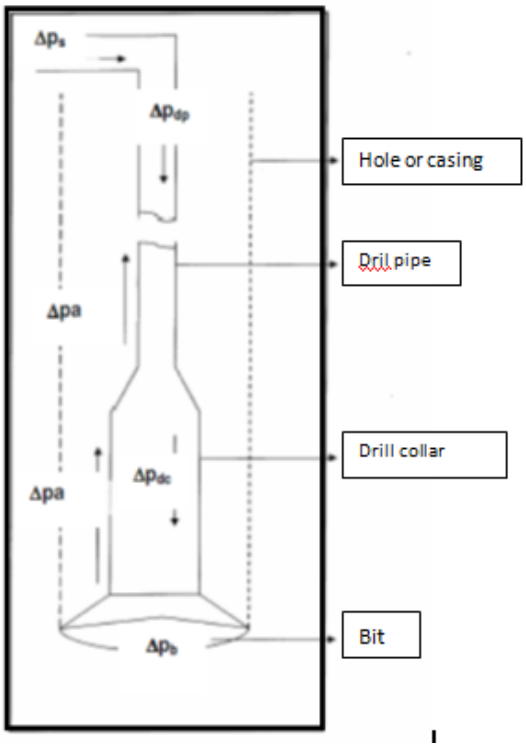

Figure 5: Diagram of the drilling fluid circulating system [17].

Frictional pressure loss is a function of several factors such as rheology behavior of the drilling fluid (Newtonian or non-Newtonian), flow regime of the drilling fluid (laminar, turbulent, or intermediate flow), drilling fluid properties (density and viscosity), flow rate of the drilling fluid (q), drill-string configuration and wellbore geometry. See Figure 5**.**

Frictional pressure losses across the bit, Δp_b:

$$\Delta p_b = \frac{156.\rho.q^2}{(D_{N1}^2 + D_{N2}^2 + D_{N3}^2)^2} \qquad (2.30)$$

Where D_{N1} , D_{N2} , D_{N3} are diameters of the three nozzles.

$$Pt = Pcs + Pdp + Pdc + Pb + Pdca + Pdpa \qquad (2.31)$$

Where

- Pt = Standpipe pressure, psi
- Pcs = Pressure loss in surface connection, spsi

- Pdb = Pressure loss through drill pipe, psi
- Pdc = Pressure loss through drill collars, psi
- Pb = pressure loss through bit nozzles, psi
- Pdca = pressure loss through hole-drill collar annulus, psi
- Pdpa = pressure loss through hole-drill pipe annulus, psi

2.3 Cutting transport model

Transportation of cuttings is a mechanism that is a vital factor for a good drilling program. In directional and horizontal drilling, hole cleaning is a common and costly problem. Ineffective removal of cuttings can result in several problems, such as bit wear, slow drilling rate, increased ECD (which can lead to formation fracturing), high torque, drag, and in the worst case, the drill pipe can be stuck.

Cuttings transport is controlled by many variables such as well inclination angle, hole and drill-pipe diameter, rotation speed of drill pipe (RPM), drill-pipe eccentricity, rate of penetration (ROP), cutting characteristics like cuttings size and porosity of bed and drilling fluids characteristics like flow rate, fluid velocity, flow regime, mud type and non - Newtonian mud rheology. The key factors for optimizing hole cleaning is a result of good well planning, good drilling fluid properties, and good drilling experience.

There are some empirical models to solve cutting transport such as [18]:

LARSEN'S MODEL: Larsen et al. focused on cutting size, angle of inclination and mud weight. This model developed to predict the critical transport fluid velocity, equivalent slip velocity, and critical velocity.

PEDEN'S MODEL: Focused on forces affecting cuttings transport in in inclined wellbore and the minimum transport velocity concept is used in this model.

RUBIANDINI'S MODEL: Rubiandini claimed that hole-cleaning problems could be mastered by defining the minimum mud rate that had a capability to clean the drilling wellbore. The minimum mud rate is a sum of the slip velocity and velocity of the fallen cuttings. The major factors that affect cuttings transport mechanism was mud weight, inclination angle, and RPM.

Kamp and Rivero: this model has presented a mechanical model for calculation of cuttings bed heights and cuttings transport velocities at different rates of penetration in horizontal wellbore by using a numerical solution.

2.4 Heat transfer in the wellbore

Schematic of drilling fluid circulating is shown in Figure 6 in the wellbore and the associated heat the differential elementr for differential element of length Δz. The figure illustrates the heat flow from the formation into the annular section through convection. This rate of heat flow by convection into the annulus is larger than the rate of heat conduction in the formation due to lower heat capacity. The heat flow from annulus will transfer via convection on the pipe surface on the inside and outside of the drill pipe. Analytical method and the numerical method can be coupled to estimate the temperature profile. Analytical method is the best method for simple geometries. In numerical method, more complexity can be imposed for the system [13].

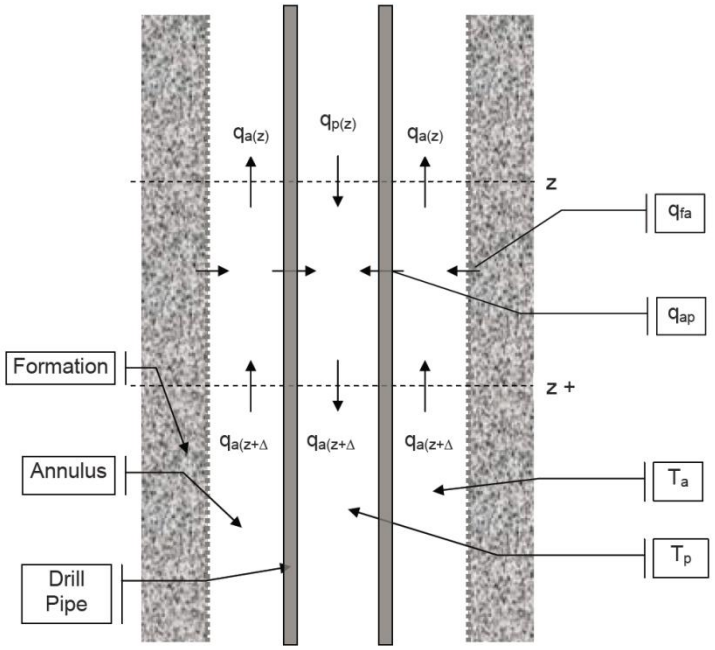

Figure 6: Schematic of Heat Balance for Fluid Circulating in a wellbore [13]

3. DrillScene Monitoring and interpretation by IRIS

The International Research Institute of Stavanger (IRIS) has developed a new drilling control and prediction system called DrillScene. The purpose of the DrillScene Advanced Monitoring Services is to detect changes in the downhole conditions during drilling operation. Such changes can represent symptoms of deteriorating conditions that are likely to evolve if no actions are taken. The symptoms can thus be used as decision support for performing remedial actions or to give an overview of the status of the drilling process.

The program uses real time models to calculate hydraulic and mechanical forces. The numerical models are automatically calibrated. By calibrating the models, handling the real-time signals and the development of deviations between measurements and predictions can detect poor downhole conditions. The software is able to predict kicks and thereby preventing blowouts. By allowing DrillScene to monitor operations continuously, people and equipment are better safeguarded during offshore drilling operations [19]. Figure 7 illustrate an example of the monitoring units.

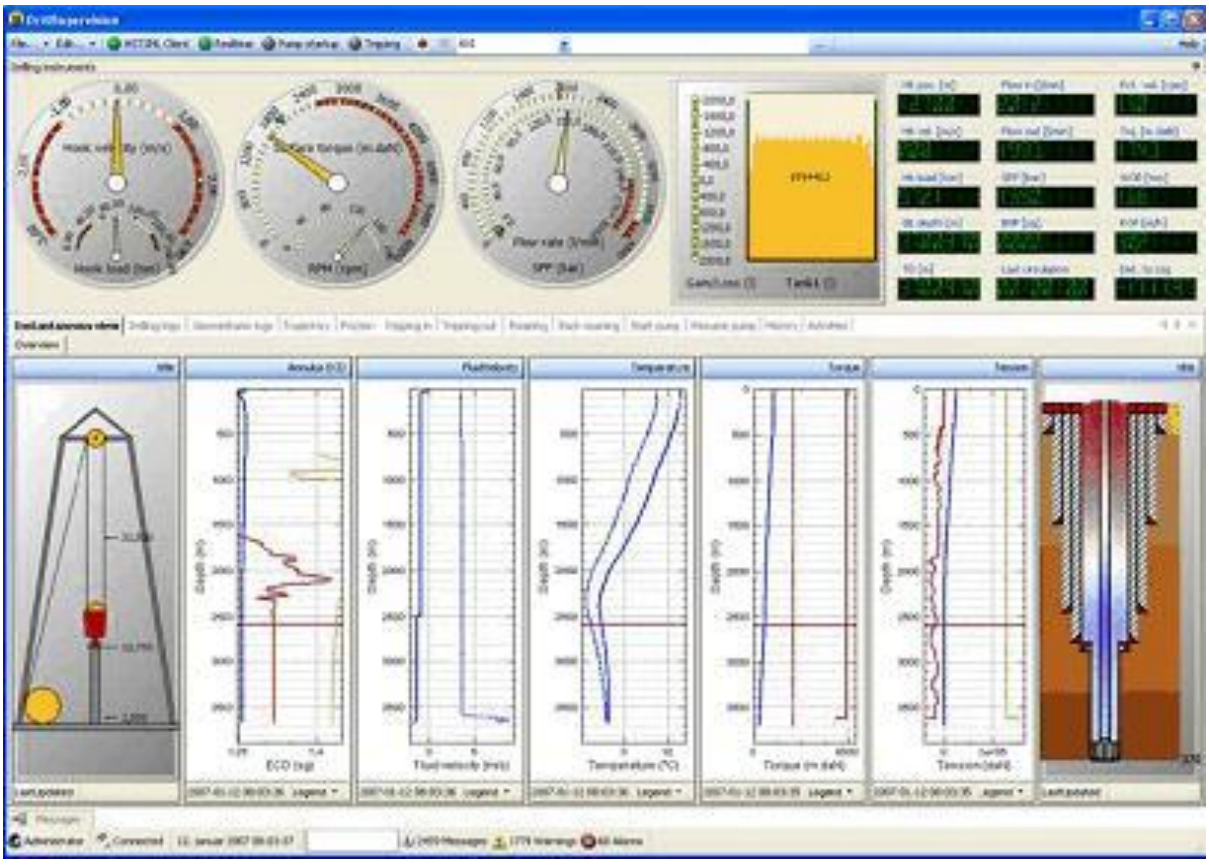

Figure 7: A schematic of Drillscene monitoring [21]

3.1 The DrillScene system

The DrillScene is a computer system which automatically analyzes real-time data in order to monitor downhole conditions. The DrillScene system utilizes the following methodology [21]:

1. Evaluate continuously the well condition by running physical models of the drilling process in real-time.
2. Detect current well conditions which can be used to calibrate the physical models.
3. Continuously perform a global calibration of all the physical models to match the recorded relevant well conditions.
4. Detect whether the current well conditions are deviating from normality.

3.2 System architecture

The system architecture of DrillScene is based on the following principle (Figure 8) [22]:

- The calculation processes running on a 24/7 basis. The DrillScene system depends on several calculation processes responsible for the computation and generation of warning or alarms.
- A middle object cache used for transfer of data between processes and the front-ends and is installed as a service on the server.
- A set of front-end (client) application which can be brought up at any time to inspect the result of the calculations.

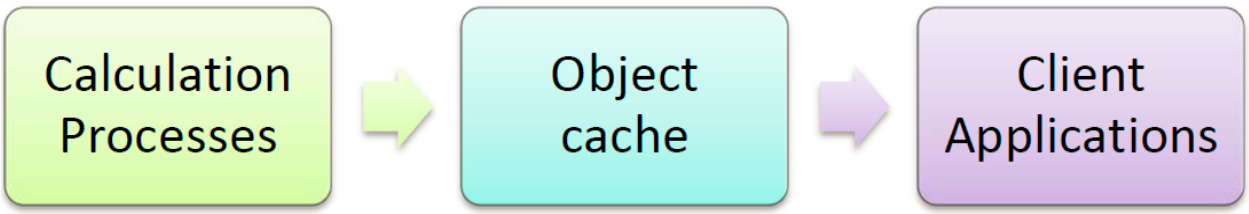

Figure 8: Drillscene's three-tier software architecture [22]

3.3 DrillScene System Setup

A system topology is presented in Figure 9. Communication between the networks is completed over the Secure Oil Information Link (SOIL) network which is divided between the Operator's rig network and the service provider's network. Several different processes are running on the calculation server. The Data Acquisition is located on the calculation server within the service provider's network. This process is responsible for reading the real-time data stream, and

interpolating the received data onto a common timeline. The object cache is acting as middle tier, through which all the processes running at one network location can communicate and exchange information. There are several object cache services running on different servers. These are mirroring the same data using replication agents which are used for synchronization [21].

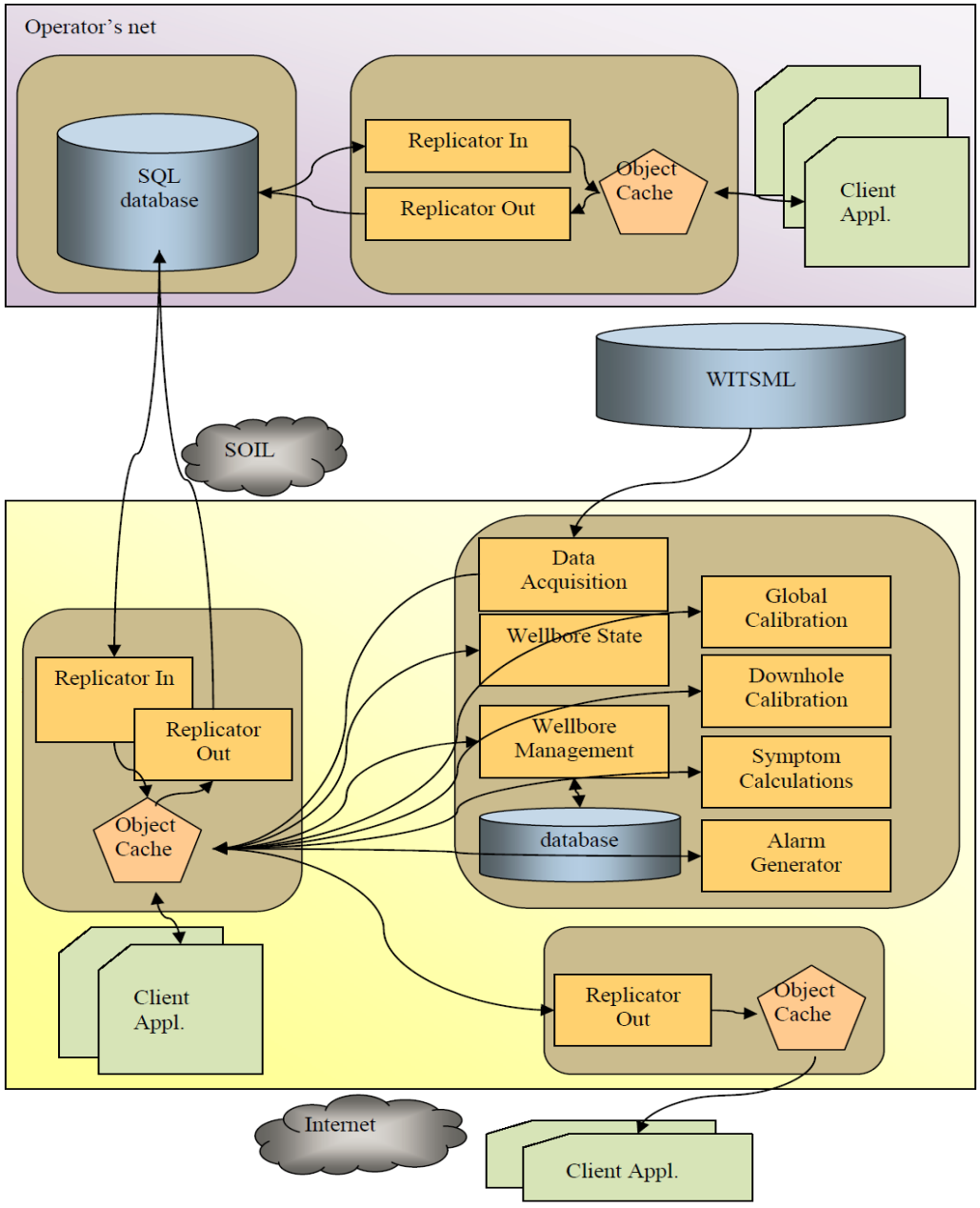

Figure 9: System topology showing a possible implementation of the DrillScene system [21].

3.4 Calculation Processes

There are several calculation processes which run as back-end processes on the DrillScene calculation server [22]:

- Wellbore Data Manager
- Data Acquisition
- Wellbore Condition Evaluation
- Global Calibrations
- Friction Factor Calibrations
- Roadmap Calculations
- Alarm Generator

3.4.1 Wellbore Data Manager

The purpose of the wellbore data manager is to maintain the wellbore description by keeping the information in the Object Cache updated. Since Object Cache is not a permanent place for data storage, there will always be an additional data source where the configuration data have to be saved.

Currently there are two possible high-speed data transfer used as a standard for storage communication of real-time data [22] [23]. These source calls:

- SQL (Structured Query Language)
- WITSML (Wellsite Information Transfer Standard Markup Language)

3.4.2 Data Acquisition

The main object of this part is to obtain the imperative real-time data from the individual sources and transfer them to object cache. Several drivers have been written, such that the data acquisition process is agreeing with the following standard data transfer [22]:

- WITS (Wellsite Information Transfer Standard)
- WITSML (Wellsite Information Transfer Standard Markup Language)
- UDP (Unconnected Device Protocol)

Most of these communication standards are consistent with the drilling real-time requirement.

3.4.3 Wellbore Condition Evaluation

During a drilling operation, the conditions in the borehole are changing continuously like temperature of the mud, the density of the drilling fluid, the fluid fronts when several fluids are circulated in the borehole and the liquid level in the drill-string when there is a float-sub.

The purpose of the Wellbore Condition Evaluation is to calculate the current state of the well by using the real-time data and wellbore description. The model can calculate the internal state of the well by applying process models such as [22]:

- Drill-string mechanical model so called torque and drag model
- Downhole hydraulic model and models like: PVT, rheology, gel, barite sag and cutting transport model
- Downhole heat transfer model to calculate the temperature of the fluids and material in the wellbore
- Surface installation model like the circulation of fluid in return flow lines, heat transfer with surface environment.

3.4.4 Friction Factor Calculations

This process uses the steady conditions monitored by the data acquisition to calculate the sliding friction, rotational friction and the hydraulic annulus friction.

For each of these frictions, the process estimates the reference friction, the current friction and its standard friction as well the acceptable tolerances for issuing warning and alarm [22].

3.4.5 Roadmap Calculations

A roadmap chart is a depth based plot representing modeled hook-load or surface torque for different friction coefficients, under some automatically defined operating conditions. The purpose of the roadmap calculation is to make the results for the roadmap charts. This process analyses the recorded steady state conditions and derive the various roadmaps which needs to be calculated using clustering of the steady state records. Then it calculates the various hook load, surface torque roadmap charts [22].

3.5 Model Calibration

A reliable modeling of the dynamics of the wellbore constantly interacts with each other; the models cannot be implemented by using of numerical models alone.

The necessary parameters for the model configuration often unknown or ill-defined, and the unknown downhole conditions have to be taken into consideration.

3.5.1 Global Calibrations

In order to cope with this challenge, a global calibration module has been designed. This process focuses on the following parameters [24]:

- Linear weight of the drill-pipes.
- Hydraulic effect on the mechanical forces.
- Frictional pressure losses inside the drill-string

3.5.2 Torque and Drag Model Calibration

This process uses steady state measurement that are sampled during rotation off bottom and when there is no friction effect on the drag [24].

The calibration that is automatically performed by the system is global, and calibrates parameters that will not change with time (e.g. linear weight of drillpipes). Figure 10 below shows an example of the effect of global calibration, the three curves on top are rotated off-bottom roadmap for three different flow rates. From the figure one can see that calculation and measurement do not match.

Linear weight of the drill pipe and the hydraulic effect are calibrated, until the difference between modeled hook load and measured is minimized. After calibration one can see much better correspondence between modeled hook load and real-time measurements (blue triangles). The three curves on the bottom of the figure show the same roadmap after calibration [24].

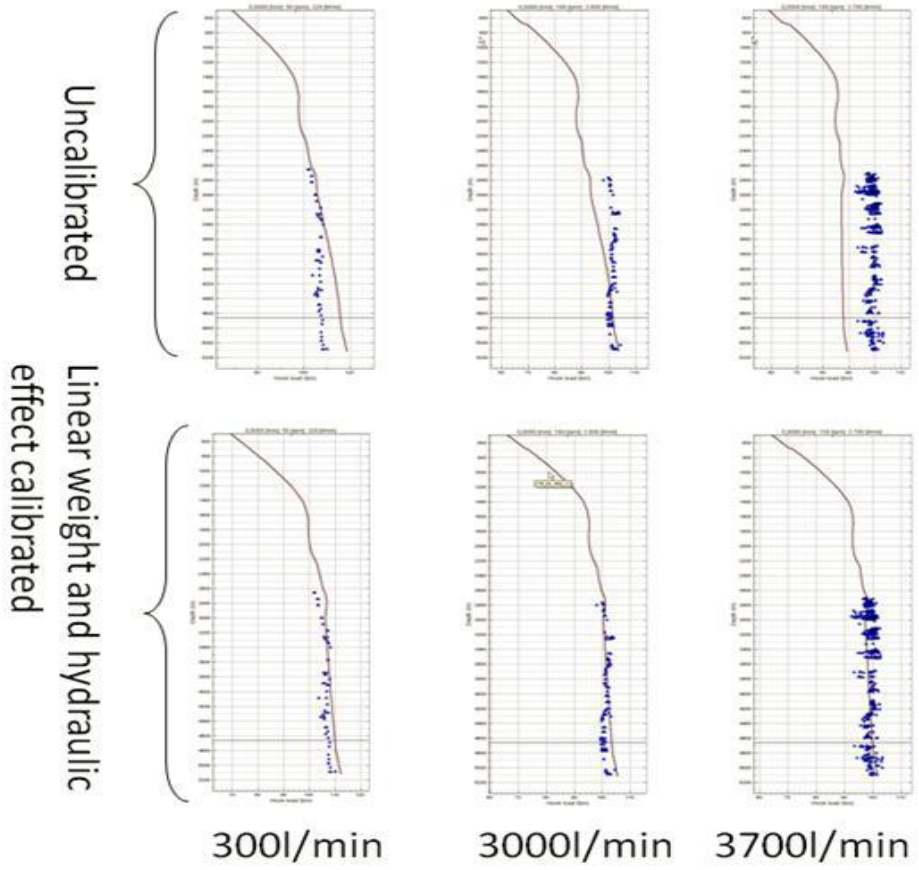

Figure 10: Torque and drag global calibration [24].

3.5.3 Hydraulic Model Calibration

The pressure losses inside the string are not dependent on external varying conditions (such as hole cleaning etc.). On the other hand, the pressure losses are dependent on flow rate and mud properties. Even with a perfect configuration of the drillstring properties, the model-based calculation may need to be adjusted to match the measured pump pressure to account for small discrepancies in the pipe roughness and geometry as well as some uncertainty of the fluid properties [24].

The frictional pressure losses within the drill-string should be calibrated to consider the possibility of wrong internal diameter. This calibration is implemented by selecting steady state measurement at various flow-rates, and by applying the necessary correction to the frictional pressure loss calculation to match the measurement stand pipe pressure (SPP). In the procedure for estimating the correction function, it is important to account for the actual temperature gradients and observed annulus hydraulic friction at the time of the SPP measurement, to remove any source of unwanted bias.

An example of hydraulic calibration is presented in Figure 11: the colored circles indicate the SPP at different depth and flow rate, and the color bends corresponds to calculated values. The color

code corresponds to the flow rate of the measurements and to the flow-rate used for the calculation (the same color coding is used). If a correctly calibrated model is used, the measurement circle should fall into an area with the same color. In that case, it means that the model predicts the correct stand-pipe pressure for the given flow-rate [24].

The left chart in the figure shows a non-calibrated model, there is no match between the measurements and calculations, while on the right plot calibration has been performed, and the colors of measurement and calculation fall in an area and do match very well.

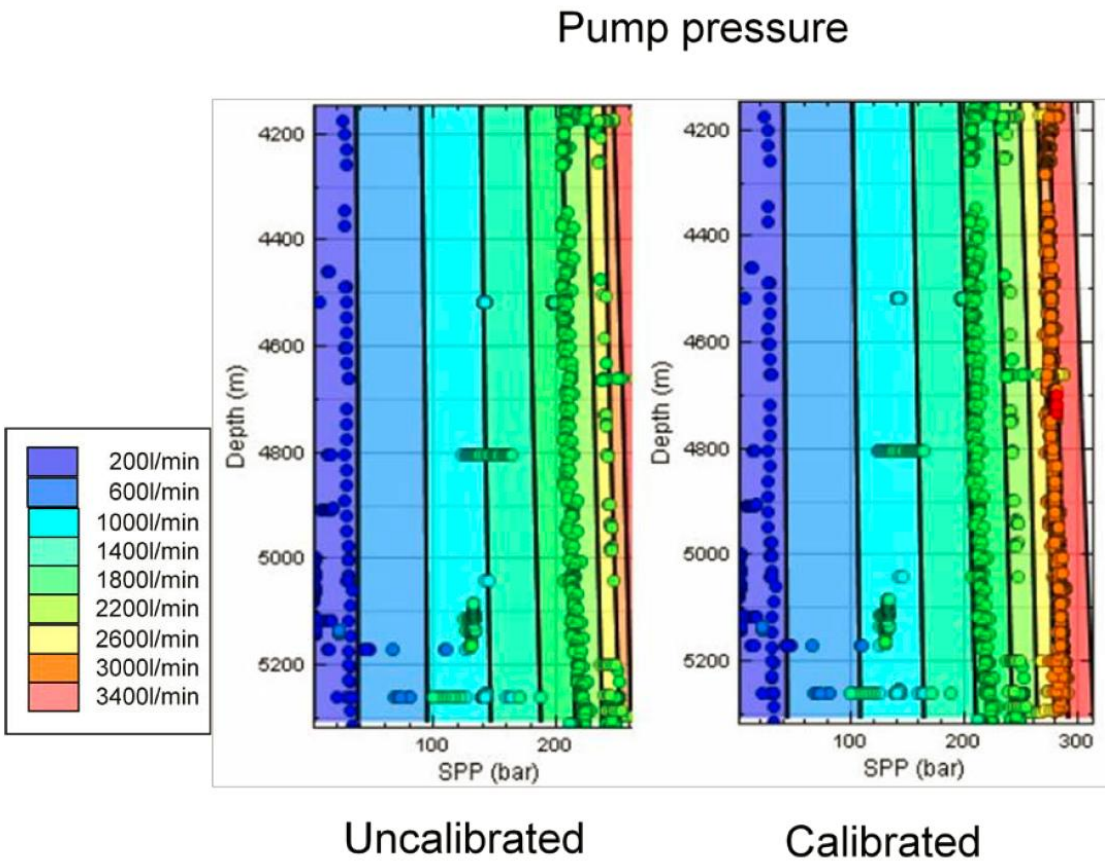

Figure 11: Global hydraulic calibration [24]

3.6 Real-time Calculation module

All calculations that need to be performed real-time are handled by the Real-time calculation module. This module gathers and monitors the real-time data continuously for every second. The following modules are presented [25]:

- Flow model with estimation
- Torque and drag model
- Diagnostics

Flow module with estimation

The flow model calculates the following parameters for each time step:

- Stand pipe pressure
- Flow rate out of the well
- Liquid level in string and annulus
- Pressure profile in drill string and annulus
- Temperature profile in drill-string and annulus
- Fluid density and velocity profile in drill-string and annulus
- Cutting velocity and transport rate

Torque &drag model

If the string is in slips no calculation needs, if the string is out of the slips there are different categories like [25]:

- Drilling when the bit is on the bottom and drill-string rotates
- Reaming , the bit off bottom downward motion with drilling rotation
- Back Reaming, upward motion with drill-string rotation
- Slack off, downward motion without drill-string rotation
- Pick up, upward motion without drill string rotation
- Rotation off bottom, bit of bottom and drill- string rotates without upward or downward motion

When the bit is on the bottom, the model uses the measured hook load and surface torque together with the references friction factor to estimate the weight on bit and bit torque.

When the bit is off bottom there are several possibilities. If the drillstring rotates, a friction factor based on the match surface torque criterion is calculated, otherwise, the match hook load criterion is used. This means that the model starts from the weight on bit and bit torque and calculates a friction coefficient to match either the surface torque or the hook load [25].

In addition, the torque &drag model also calculates side force, helical buckling limit, sinusoidal buckling limit, tension and torsion profile [25].

Diagnostics

The available real-time parameters are continuously analyzed by DrillScene, such that early warning signs of deteriorating downhole conditions can be detected. The correct interpretation of the problems needs an analysis of multiple symptoms, which can be a challenging task for computer system. A computer system can assist in performing calculations which can be used in this analysis, as well as detecting the different symptoms. Since various down-hole problem may lead to similar symptoms, human interpretation will still, be required to determine the correct proactive action.

In this part of thesis will focus on the Drillscene's different parameters, where one can observe symptoms and changing in downhole conditions before any major drilling incidents occurred. The following symptoms are available:

- Hook load, Block velocity
- Surface torque
- Road maps
- Friction plots: sliding friction (based on hook load), rotational friction (based on surface torque), annulus friction (based on downhole ECD).
- Downhole Equivalent Circulating Density (ECD)
- Stand Pipe Pressure (SPP) and Stand Pipe Pressure Deviation
- Free Rotating Weight Deviations (FRW)
- Relative volume and cuttings flow rate (Gain/loss): measurement of abnormal changes in hook load when the drill-string is not moving axially but is rotating

3.6.1 Hook Load, Block Position and Block velocity

Figure 12 shows the block position, block velocity and hook load measurement, the block velocity displays both the measured velocity (blue curve) and the maximum velocities as calculated by the system to avoid damaging swab and surge effects (red for upward velocity and yellow for downward velocity). On the hook load chart the blue curve is measurement hook load and the green curve is modeled hook load and the green region area is acceptable hook loads. The calculated hook load is a function of the Revolution per minute (RPM), friction and the flow rate. Hook load is only modeled when off bottom. Whenever the measured value is above the green region area, a red band will be displayed to indicate that the measured hook load is above expected (over- pull). When the measured hook load is below the green region area, an orange band will be displayed to indicate that the measured value is below expected (set-down) [22].

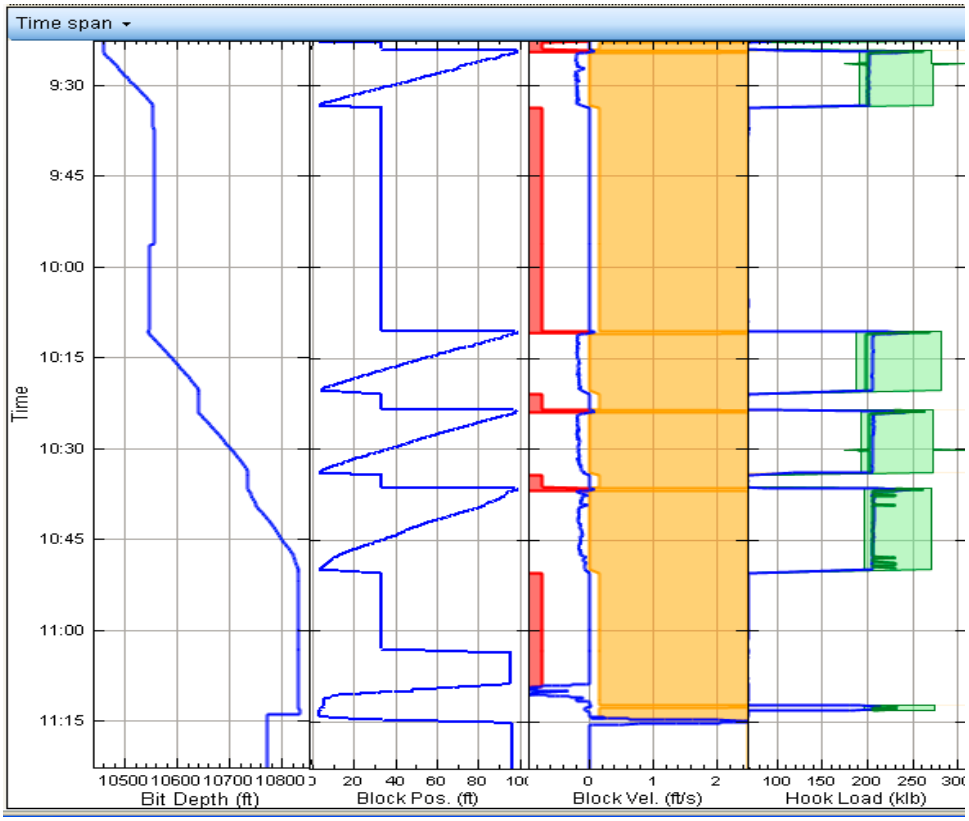

Figure 12: A chart of block position, block velocity and hook load [22].

Figure 13is time based log that shows the evthe holeion of hook load while pulling out of hole, towards the end of the cleaning process during the pull of the hole around 12:00, the system starts to report that the downhole condition is not good. At 13:15 as the figure shows the measured hook load (blue curve) is deviated from the expected trend curve (green curve). This is clear signs of a pack-off situation. According to the paper [24] the pull out of the hole process has been stopped and they decided to run in hole and clean before a new pull out of hole. The green curve and the green region area are predicted and acceptable values based on model calculations. The red regions are places where the measured values exceed tolerances. The yellow region area is acceptable velocities [24].

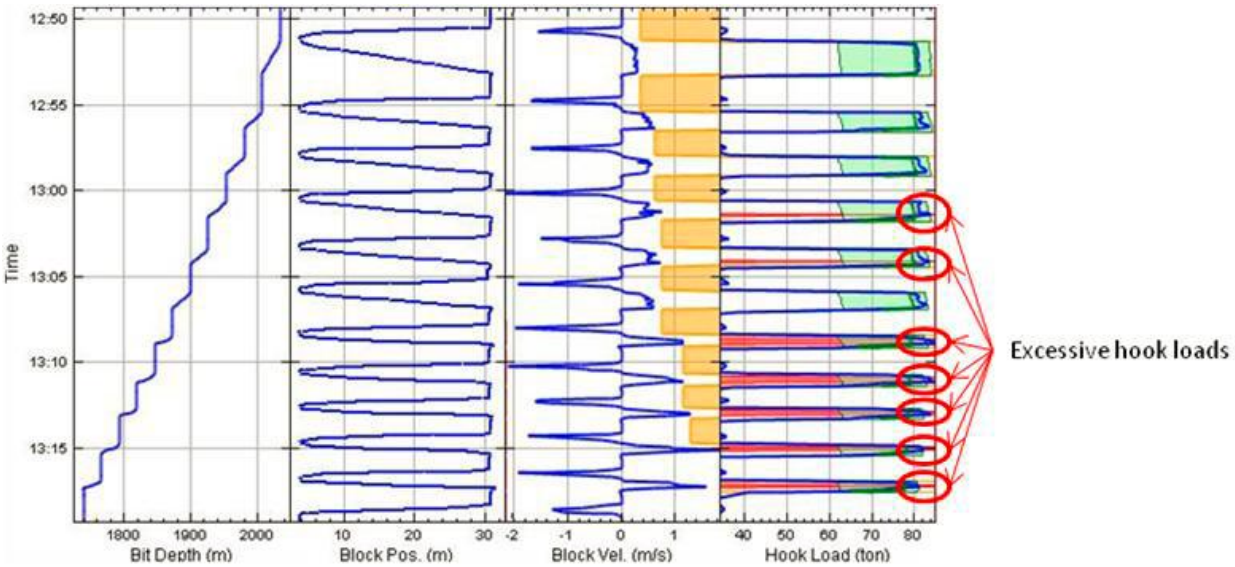

Figure 13: The evolution of hook load while pulling out of the hole [24].

3.6.2 Surface torque

The blue curve represents the measured value. The green curve represents the calculated surface torque. The calculated surface torque is a function of the current rotational friction, which in turn is absorbed both viscous effects and effects of different RPM. The surface torque is only modeled when off bottom. Whenever the measured value is above the green band, a red band will be displayed to indicate that the measured surface torque is above expected. Whenever the measured hook load is below the band, an orange band will be displayed to indicate that the measured value is below expected, see Figure 14.

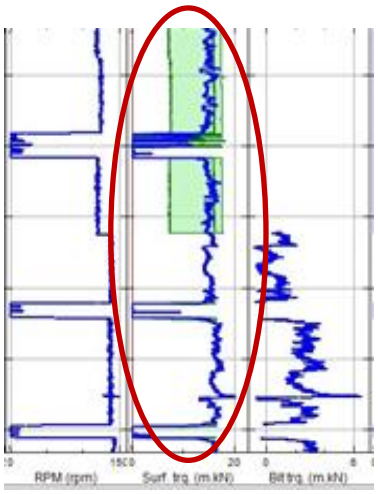

Figure 14: The surface torque window.

3.6.3 Roadmaps

The roadmaps are matched for trend observations, and they allow a direct comparison between measured and modeled values. A roadmap charts are a depth based plot representing modeled hook-load or torque for different friction coefficients, under some automatically defined operational conditions (block velocity, rotational frequency and circulation rate). The corresponding measurement (hook-load or surface torque) are displayed on the chart, and one can thus monitor easily the evolution of the studied sliding friction or rotational friction [22].

Warmer colors represent more friction, and the solid green curve represents the current friction with its standard deviation plotted as a green hashed area.

Figure 15 shows a run in hole (RIH) roadmap that indicates a good downhole conditions. DrillScene detects automatically the different fill-pipes, and includes them in the roadmap calculations. The mud inside the drill string has important effects on buoyancy, then on the measurement hook load. Whenever the drilling parameters are kept constant for a certain depth, the measurement points should at least follow a constant friction level.

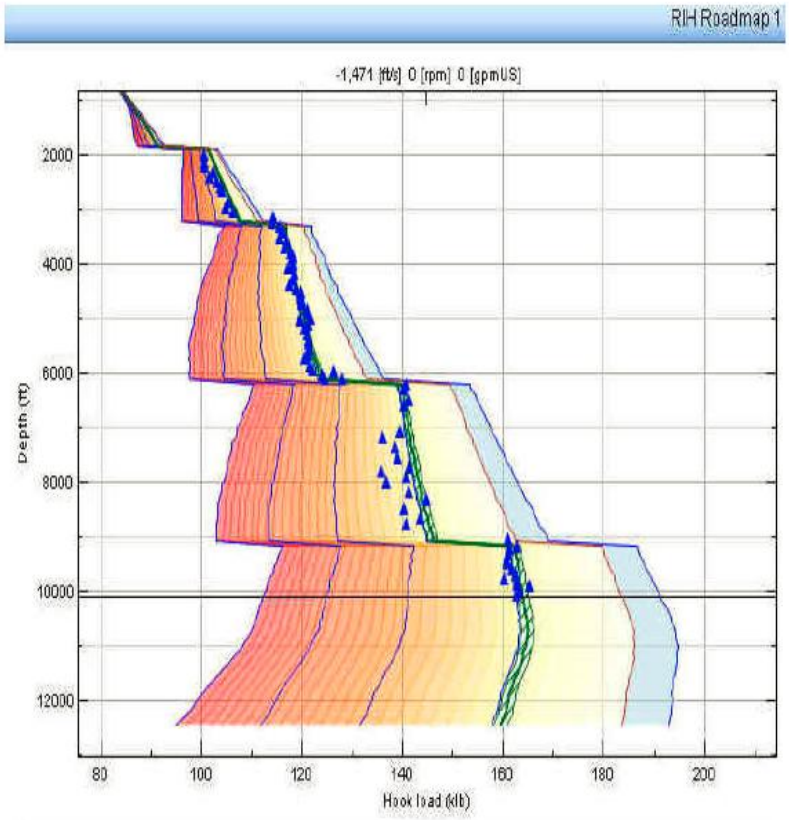

Figure 15: A RIH roadmap taking into account the filling of pipes [22].

Figure 16 shows a trend change on roadmap during POOH. If the current drilling parameters are leading into poorer hole cleaning, one can normally see a trend where the measurement points are falling in at higher frictions, associated with higher friction in the wellbore. The left side

chart measurements following a single friction line and on the right hand side one can see that trend suddenly deviated this indicates that the hole conditions were not in normal condition.

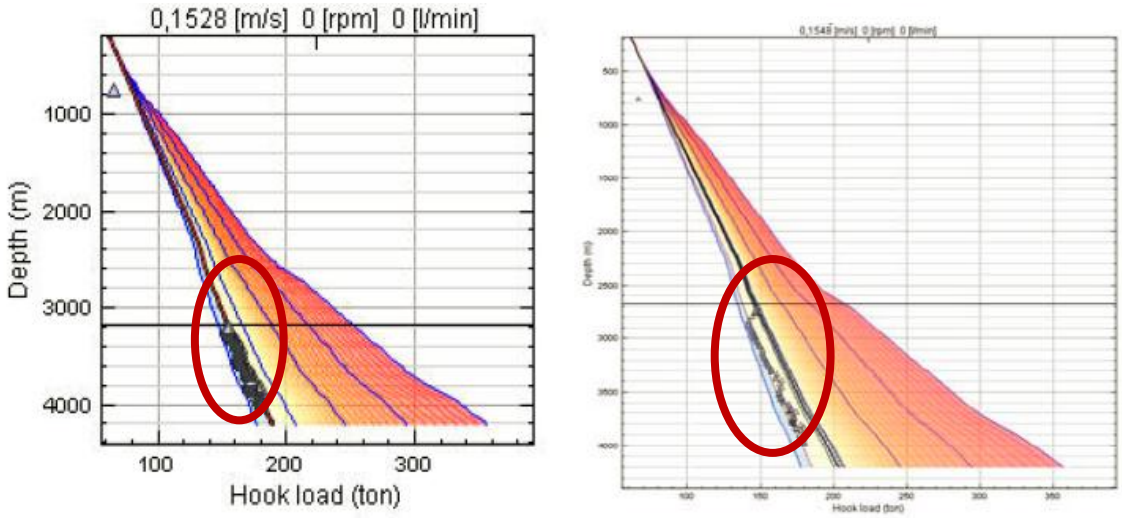

Figure 16: Change of trend on a POOH roadmap [21]

3.6.4 Friction plots

Sliding friction: Drag forces act against the displacement in Sliding friction *during* lifting up or slacking off the drill-string. These friction forces are function of a kinetic friction that depends upon the mud properties and the mechanical properties of the contact surface [21]. Sliding friction is back-calculated from the difference between the measured- and modeled- hook load and accounting for hydraulic effects from different flow rates. The sliding friction is calculated whenever the bit is off bottom, without rotation during steady state. Downhole condition is no optimal when current measured friction is larger than the reference friction. DrillScene is discriminating between friction when sliding up or down, shown by red and green lines and dots. If there is a significant difference between the frictions up and down, this can be an indication of poor hole cleaning.

Rotational friction: when rotating the drill-string, the Coulomb friction is working against the rotation and causes an increase of the momentum along the drill-string (from bottom to top). The rotational friction is basically a static friction (because the pipes are rolling on the contact surface) and therefore can be higher than the sliding friction [21]. Rotational friction is in fact a correction to the model made in order to have the model match the measured surface torque. This correction is accounting for both viscous and mechanical effects, and is thus not a pure mechanical friction. The rotational friction is calculated whenever the bit is rotated off bottom, without significant axial movement.

Annulus friction: the downhole pressure returned by a pressure while drilling (PWD) tool can be used to detect unexpected pressure losses during circulation. The system calculates a fudge factor applied to the pressure loss gradient calculated along the annulus in order to get a match with the measured downhole ECD (Equivalent Circulating Density) [21]. , if the measured PWD value is above the modeled value due to e.g. cuttings loading, the values will be plotted in the Annulus friction max trace. Increasing trends of the Annulus friction can be related improper cuttings transport.

During drilling process the friction plots should be constant and stable in normal conditions. Here will give some examples to show how the friction plots use to predict downhole conditions.

Figure 17 below shows tow sliding friction plots and hook load roadmap at 2 hours interval. Those tow sliding frictions is calculated during POOH sequence. The first one all parameters indicated that the hole is in good condition and sliding friction is around 0.1 (Coulomb friction) and trend not deviated to the higher values. The left hand chart shows the evolution of the sliding friction and the right hand plot shows the hook load road map measurement. In this plot the brown circle markers correspond to actual measurements and the orange and the red area shows different levels of the warning area. On the sliding friction chart the blue curve is close to the green region that it is optimum reference value, and this shows that the hole is in good conditions. On the road map chart, the raw black markers (pick-up weight) on the hook load in the normal condition should be in the same trend and on the expected calculated area [21].

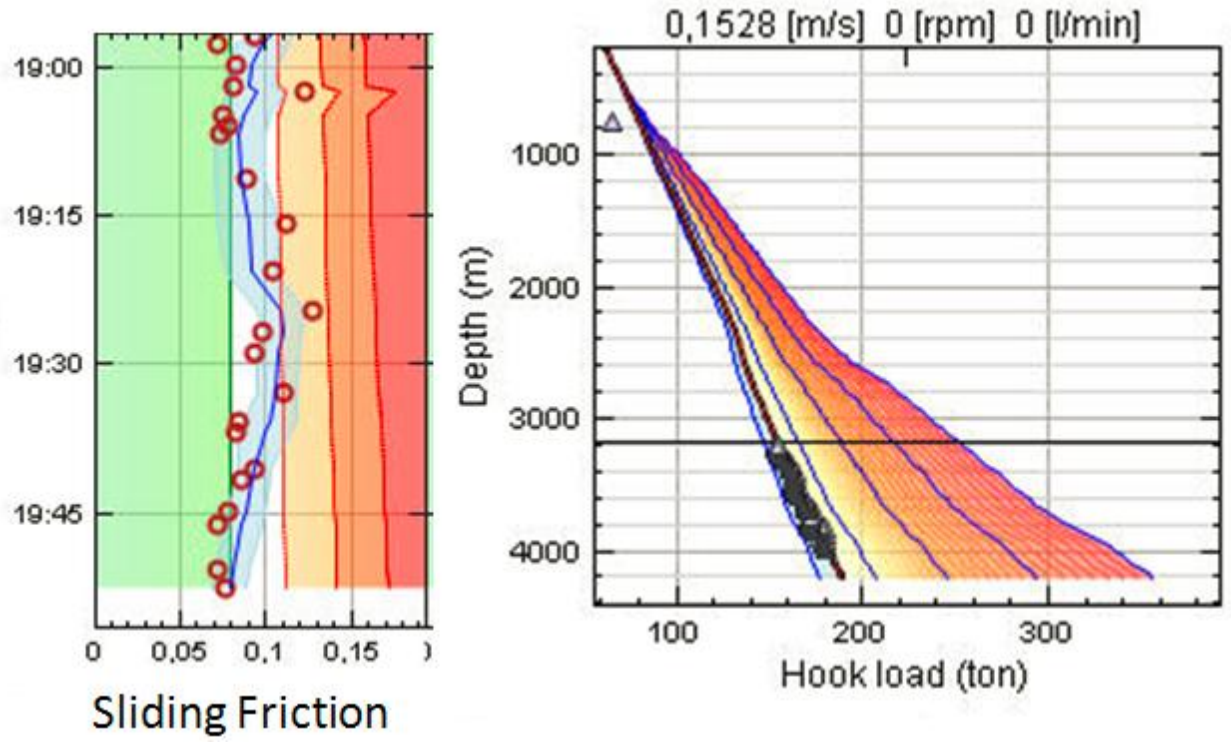

Figure 17: Sliding friction and Hook load plots in the first part of the pull out of the hole [21].

In the Figure 18, the sliding friction and the hook load deviated from the expected trend. According to this information, it is a sign of poor downhole conditions and a warning alarm has been sent to the offshore and first over- pulls occurred approximately 30 minutes after the friction increase was detected. From the figure the sliding friction (left side) began to increase and deviate from their path at 22:00, which corresponds to a rapidly increasing friction and this enters the first level of the alarm. The pick-up weight plots on the right side (Hook load) deviate from the modeled trend, it means lower than expected area [21].

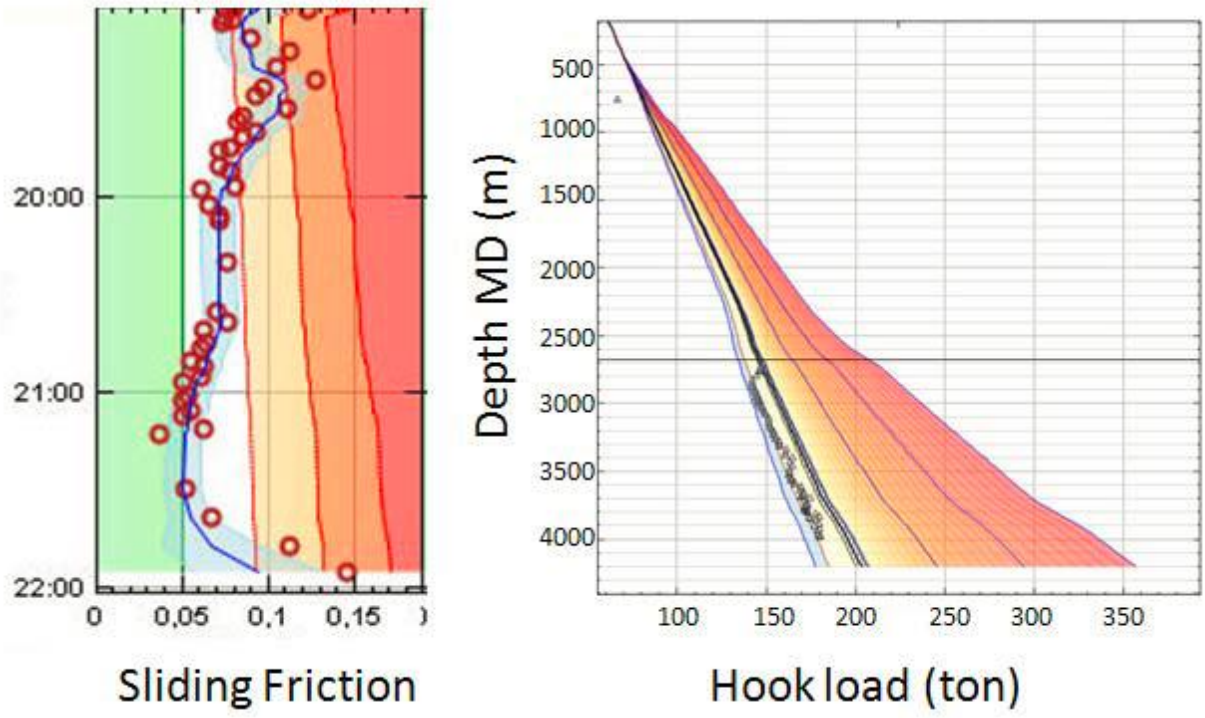

Figure 18: Sliding friction and hook load roadmap during over-pull situation [21].

An example is taken from the North Sea filed in 12 ¼ "section. To clean the well it used the maximum flow rate and high rotational velocity. The drill string is pulled out of the hole slowly, about 6 min per stand. During POOH, the hook load evolution is abnormal and changing trends in sliding friction to the high value (Figure 19). At the same time the Equivalent Circulating Density (ECD) plot shows that the swabbing pressure is under the collapse pressure of the open hole formation (Figure 20). The first over pull experience after 5 hours, this problem continues several times and numerous of pack-off and overpulls happens during 7 days. The well had collapsed while pulling out of the hole and finally the section was plugged and sidetracked.

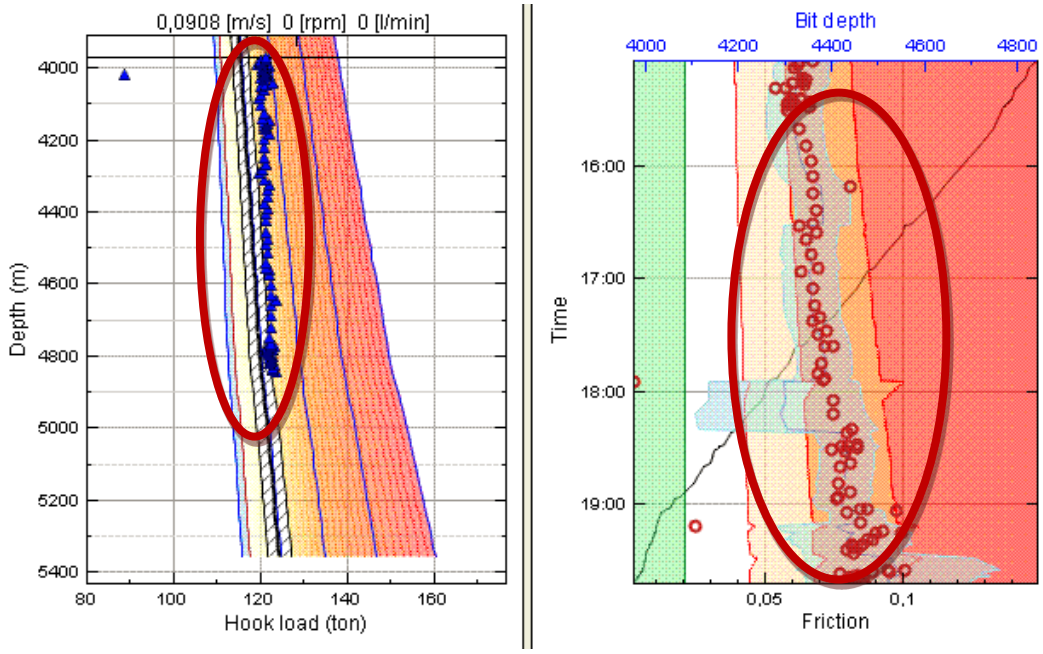

Figure 19: The left hand side is hook load evolution compare to the calculated value and right hand side shows the sliding friction deviation [21].

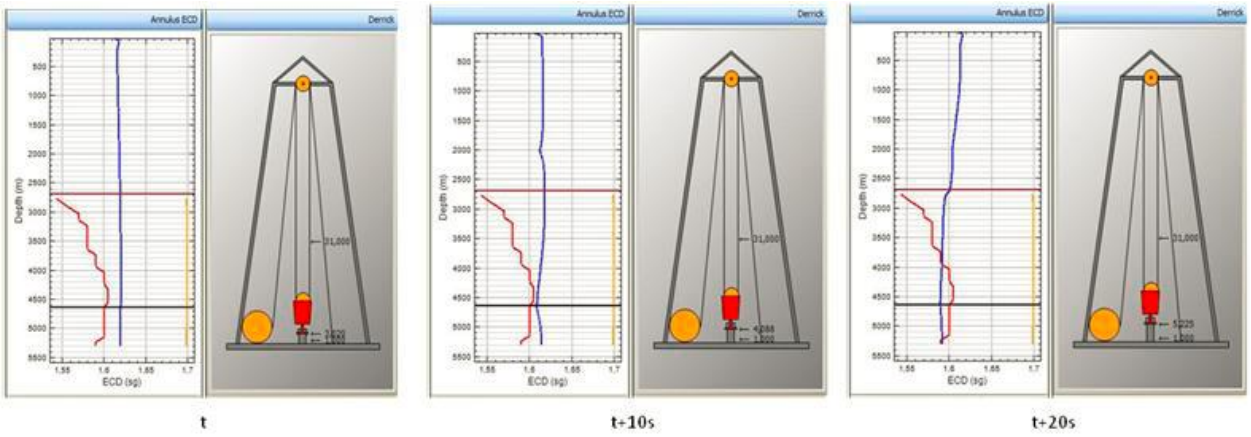

Figure 20: The downhole pressure (ECD) is below collapse pressure while pulling up the string [21].

Another example is taken from the drilling of a 17 ½" section on the North Sea field. The rotational friction at the end of the drilling of this section is high, but after cleaning the hole before tripping out, the rotational friction stabilized.

Figure 21 shows a back-reaming three stands, the rotational friction went up to 0.40 and shortly later after 1 ½ hour the friction decreases an stabilizes at 0.3 with a better standard deviation. In

normal conditions the rotational friction trend should be between the 0.4 and 0.25 as the figure shows.

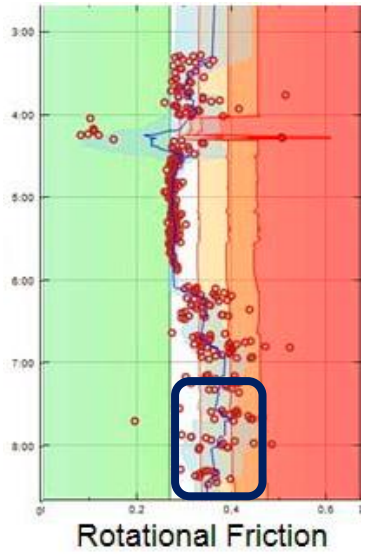

Figure 21: Rotational friction increases but after 1 1/2 hour started to decrease (7:30) [21].

Figure 22 shows that the rate of the rotational friction has been larger when getting close to the casing shoe, it constantly increases up to 0.55. While cleaning the casing, the rotational friction decreases to normal values (0.33). In this example no actions have been taken and no time has been lost. This can be counted as a false positive for the monitoring system. However, the fact that no incident occurred during this operation is largely attributed to the very low inclination of the well in this section [21].

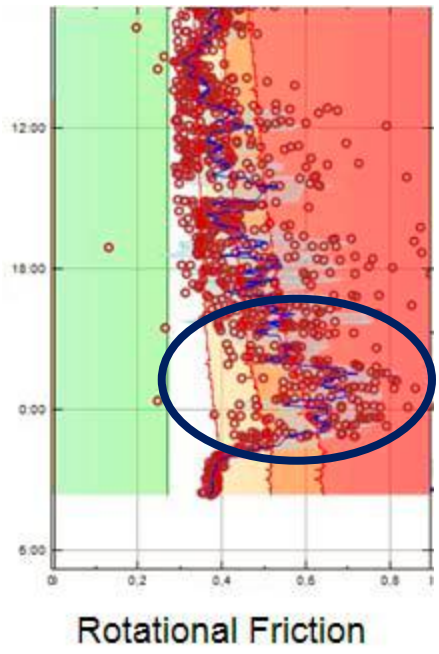

Figure 22: The rate of rotational friction increases up to 0.55 [21].

3.6.5 Downhole Equivalent Circulating Density (ECD)

The circulation of drilling fluid in the annulus is causing pressure loss. By integrating the pressure losses from the top of the annulus down to the bottom of the hole, one can determine the circulating pressure at any depth of the annulus. This pressure can also be translated in equivalent mud weight (EMW) and is often referred to as the ECD (Equivalent Circulating Density) [24].

The ECD profile is probably the most relevant when it comes to detection of downhole condition deterioration. The pressure losses along the annulus depend on the fluid velocity, drill-string velocity and rotational velocity and also on the drilling fluid properties (density, viscosity) [24].

The cutting concentration changes the mud density; therefore have an effect on the pressure losses along the annulus. In addition, the cross section of the annulus at a given depth is determining the bulk velocity of the fluid for a given flow rate and thus has a large impact on the pressure losses at that depth [24]. Cuttings bed reduces the annulus area and thereafter causing additional pressure losses.

To keep the pressure profile within the available pressure window, it is important to consider the whole open hole pressure profile. Figure 23 shows the wellbore schematic together with the annulus ECD and ESD profiles. The green curve is ESD that is seen to be at the border of the available pressure window. This is due to the high temperature inside the wellbore, which will give a lower density and therefor also lower ESD than expected. The current situation, which includes circulation, is represented by the blue line, which is the ECD. The red area on the graph represents the pore-pressure and yellow area represents the fracture pressure. The horizontal

purple line represents the last casing shoe, while the black horizontal line represents the current bit depth. The model will be calibrated against the PWD whenever this is available, and the PWD measurements are shown as a blue cross close to the bit. Whenever the modeled ECD crosses either the red or the orange area, the traffic light alarm status will turn red.

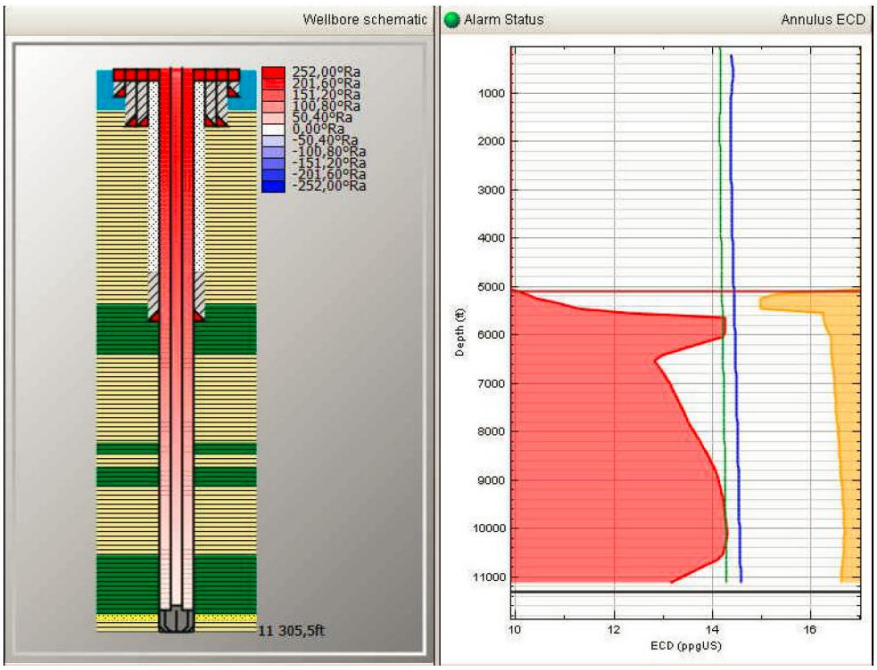

Figure 23: Low ESD (green curve) and ECD (blue curve) [22].

Figure 24 shows the end of the section when drilling. During drilling, the downhole pressure began to go below the collapse pressure at connections. A warning concerning this decrease in down hole pressure was sent to the drilling support team, but no actions were taken. When total depth (TD) was reached, the well was cleaned by using the maximum flow rate and rotational velocity. During the well cleaning, the downhole ECD was above the pore pressure gradient. Furthermore, during the clean-up procedure a steadily increase in top drive torque was observed. The well began to pack- off and five hours after the flow check, the drill-string was completely stuck. A decision was made to cut pipe right above BHA. The well plugged and a side-track was drilled. After the stuck-pipe it took 9 days to reach same depth [21].

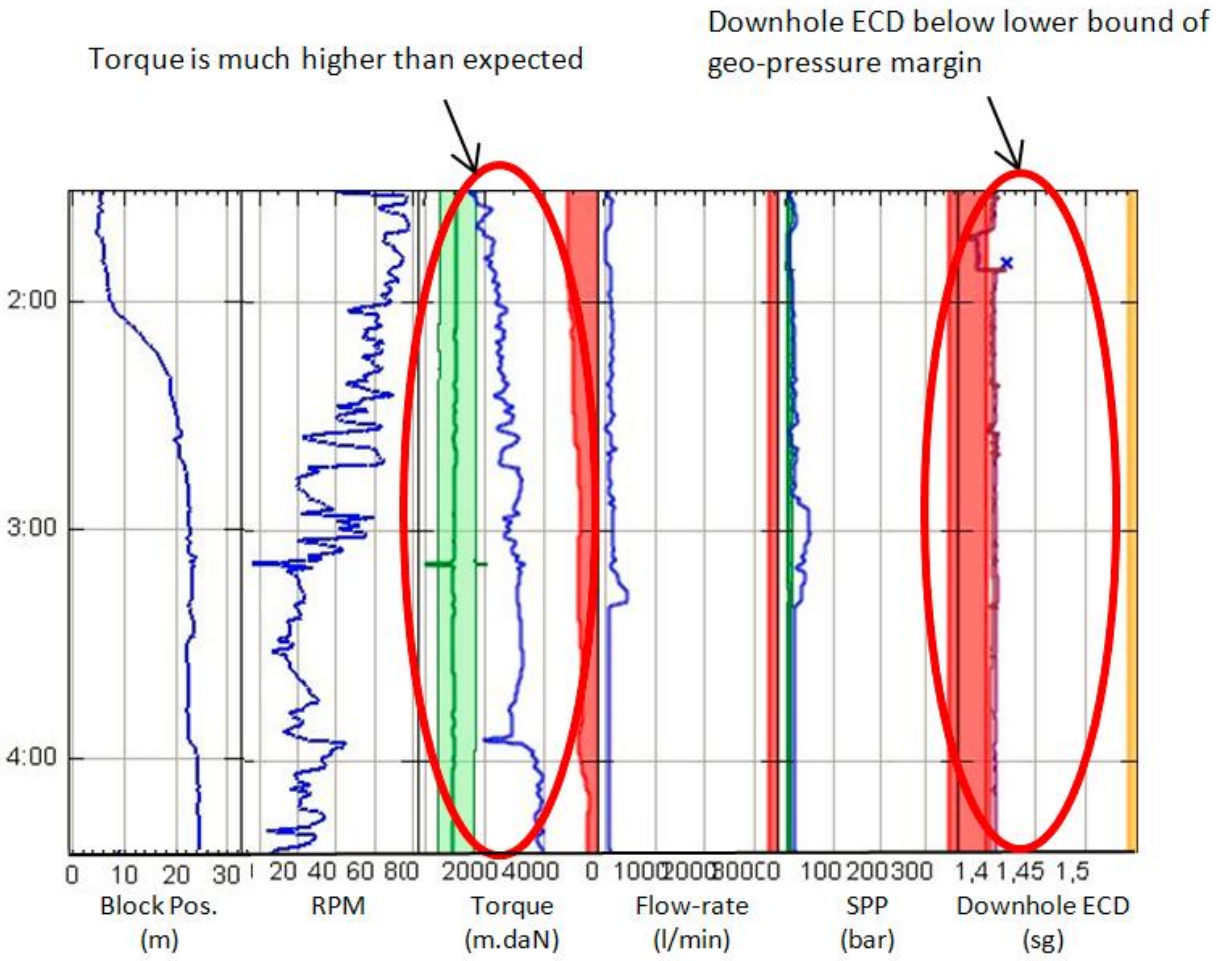

Figure 24: Time based log that shows increasing of the torque after flow check and ECD above collapse gradient [21].

Figure 25 shows another example of time-based log of the 12 ¼" section. During drilling, when nearing the end of the well (TD), splintery cavings were observed in the shaker room and return gas began to increase. Also, downhole ECD went below the pore pressure gradient because they were already drilling with low ECD compared to the geo-pressure boundary limit. Because of this low ECD, there were larger risk for a hole collapses problem or formation fluid influx.

The torque started to increase when the flow- check started. The driller controlled the situation by starting the mud pumps. The concern was hole collapse, but when mud pumps came on, the mud density increased to 1.43sg, thus the well became stable and possible hole collapse was avoided [21].

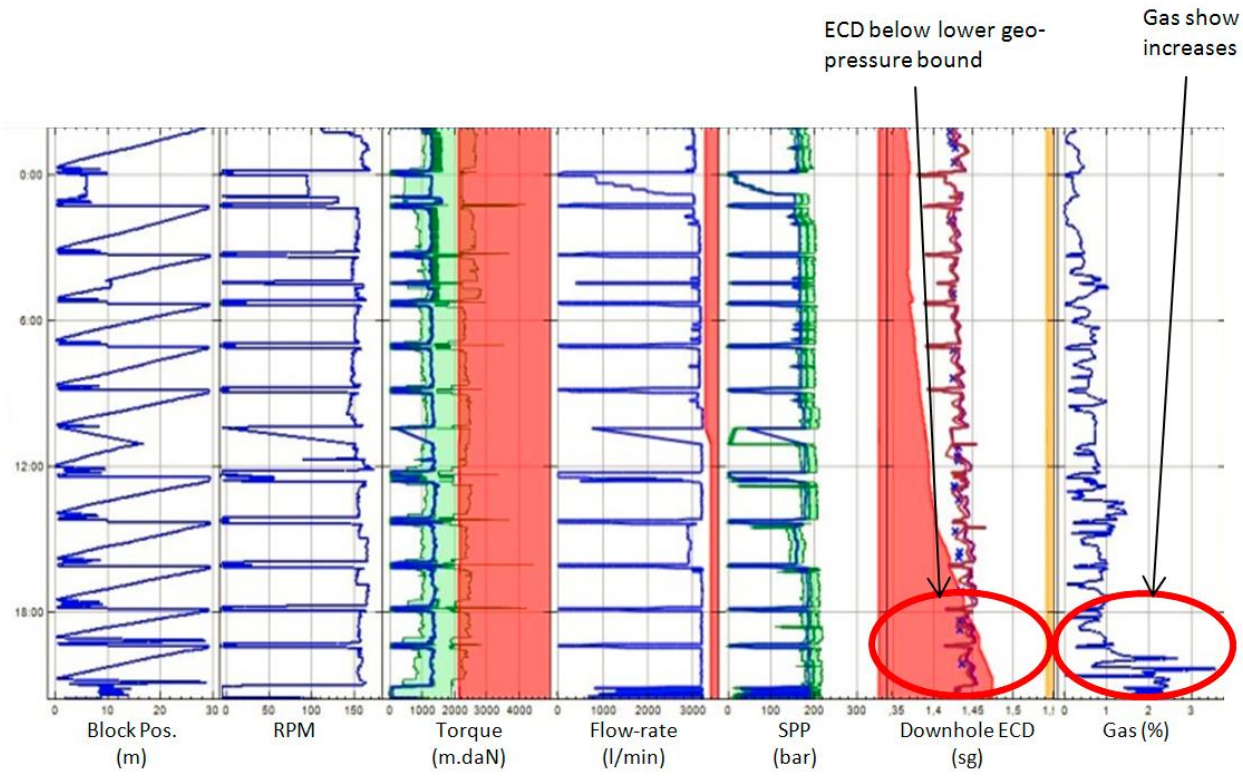

Figure 25: Geo-pressure window based the observation of cavings and gas [21].

3.6.6 Stand Pipe Pressure (SPP) and Stand Pipe Pressure Deviation

Stand pipe pressure (SPP): The global calibration of the pressure loss through the drill-string is important in order to use the Stand Pipe Pressure (SPP) variables as a source of information about the downhole pressure instabilities. By taking the ratio between the observed pump pressure and the expected SPP calculated with the calibrated hydraulic model, it is possible to estimate the abnormal change of the SPP [24].

Changes in the flow-path are affecting the SPP, like the opening of an under-reamer or a circulation sub, a pipe wash-out, or plugged by nozzles. The annulus pressure on the bit is a boundary condition of the drill-string hydraulic system, when there is no modification of the flow- path, the variation of downhole pressure is reflected as SPP variations [24].

Figure 26 shows an abnormal increase of pump pressure. In this chart the blue line represents the actual measurements, while the green line and associated semi-transparent region are expected values based on models. The green curve is independent of whether the bit is on the bottom or not, and should therefore always display a modeled value. Note that some discrepancies between the measured values and the modeled values will likely appear upon rapid acceleration of the pumps. This is due to effects of e.g. the fluid compressibility that is normally only roughly described since this is hard-to-get data. Whenever the measured value is above the green band, a red band will be displayed to indicate that the measured SPP is above expected [24].

When the measured hook load is below the standard region area, an orange band will be displayed to indicate that the measured value is below expected. Typically the red and orange bands will be displayed when the pumps are accelerated due to the discrepancies. From the figure at the beginning (the first 10 min.) the observed SPP and the expected curve (green curve) are matching perfectly, but after 15 min. the SPP is higher than expected value (around 20bars)[24].

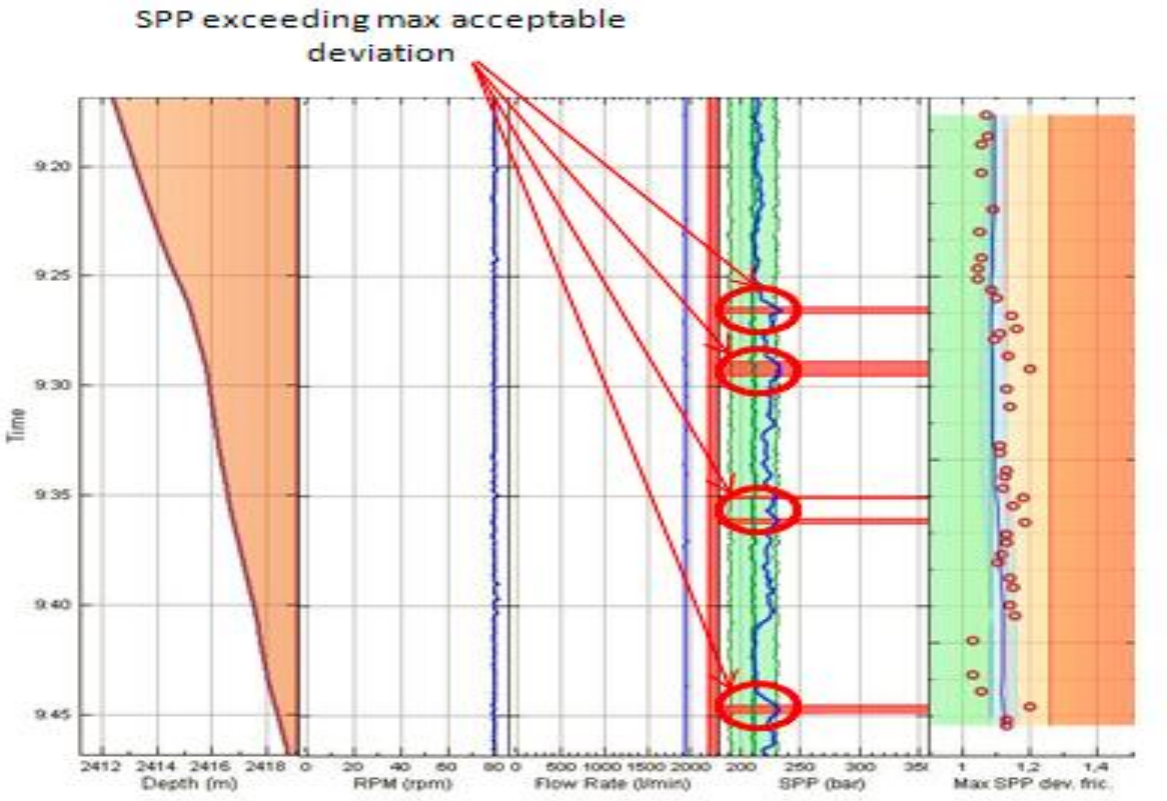

Figure 26: An abnormal increasing of the SPP related to the increasing of downhole pressure [24].

Stand pipe deviation (SPP): SPP deviation is representing the maximum deviation between the measured and modeled SPP values. That is, the largest deviation below the modeled value for a certain time span is plotted in the SPP deviation min trace, while the largest deviation above the modeled value is plotted in the SPP deviation max trace. If the measured SPP is consistently above the modeled SPP, all points will end up in the SPP deviation max trace, and the opposite if the measured SPP is consistently below the model [21] [24].

Figure 27 shows the SPP deviation charts during the drilling of the cement plug. The SPP deviation has been unstable and above the expected value. On the figure as shows, the SPP chart did not show any deviation until 1 hour before the first pack-off, where the SPP deviation increased substantially to the maximum part.

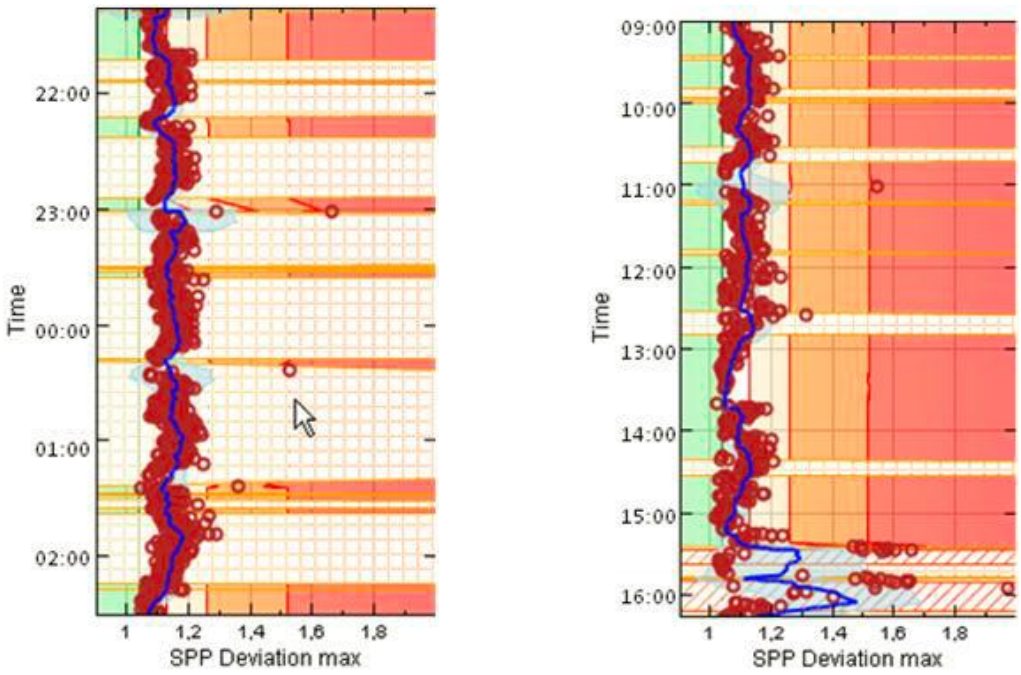

Figure 27: SPP Deviation during drilling of the drill-out cement [24].

3.6.7 Free Rotating Weight Deviations (FRW)

FRW represents the difference between the modeled hook load and the measured hook load when rotating off bottom without significant axial movement. There were no or minimal drag forces and as a result, the friction was assumed to have no influence on the measurements. The wellbore conditions have an impact on the measured weight of drill string due to the variation of the mud weight along the drill- string and inside annulus. The pressure, temperature gradient and cutting concentration along the wellbore are changing buoyancy effect; it is therefore important normalizing measured values to make the comparison at different depths and a time interval. Please see Figure 28.

Several effects can influence the free rotating weight [24]:

- The weight of cuttings on the drill-string.
- Cuttings falling down along the annulus like an avalanche because of their accumulation causing downward force on the drill-string and therefor increase in hook load.
- Restriction of fluid passage by cuttings accumulations in the annulus which causes the drill string to behave as a piston and lifts it up if circulation is continued, this causes a drop of hook load.

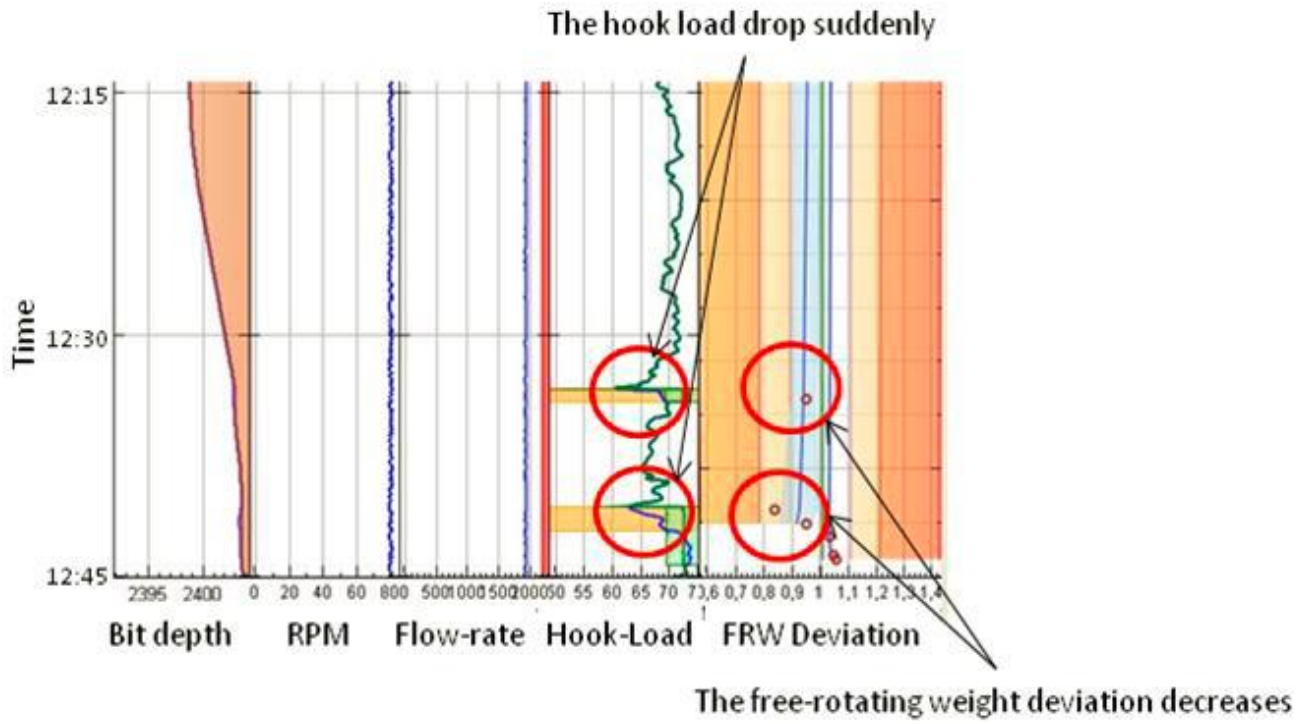

Figure 28: The two obstructions are causing the drill-string to be lifted up [24].

The Figure 29 below shows a pack-off situation, as the figure shows around 12.30 there are a few lifts up conditions, the situations became normalized and stable. At time interval 15:00, the number and amplitude of lift conditions started to increase, which gives a warning sign that the downhole conditions are seriously deteriorating one hour before the pack-off situation. If an obstruction is occurring, the drill-string may be lifted up as a piston and therefore the hook load reduces [24].

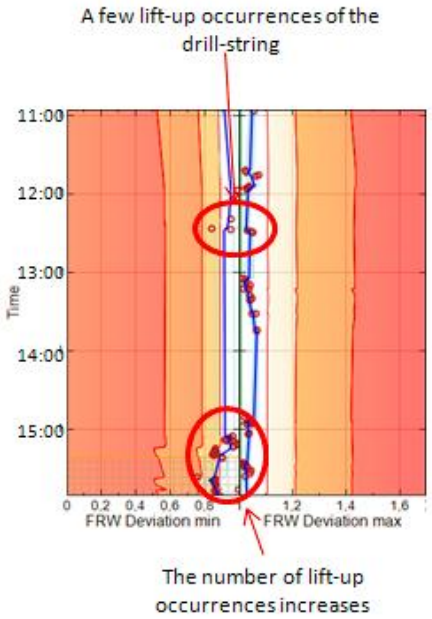

Figure 29: A pack-off situation shows in free rotating weight deviation chart [24].

:

3.6.8 Relative volume and cuttings flow rate

The variation of active volume can be useful in many ways. It might be used as primary information for detecting kicks or losses to the formation, and monitoring the cuttings removal. When cuttings are out of the hole, the active volume reduces due to wet mud taken with it some of that volume. Depending on the rate of penetration (ROP) and flow history, one can calculate the volume of cuttings produced by the bit. By using a cutting transport model, it is possible to estimate the movement of the cuttings along the wellbore as a function of the flow-rate and rotational velocity of the drill-string. DrillScene is using the calculated cuttings flow rate to model the active volume [24].

In the normal conditions when there are no losses to the formation and no formation fluid influx, the variations of active volumes are reflecting the cuttings removal from well. When cuttings arrive at the surface, a film of mud is sticking around the cuttings causing a certain amount of mud loss in the active pits. The active volume decreases when the flow rate is increased, and increases when the flow rate is reduced. In Figure 30, the time based log shows the expected cutting flow rate and the relative active volume variation between each mud pump start up. The DrillScene software uses expected cuttings volume separated at shakers to model the expected volume drop in the active with a color band [24].

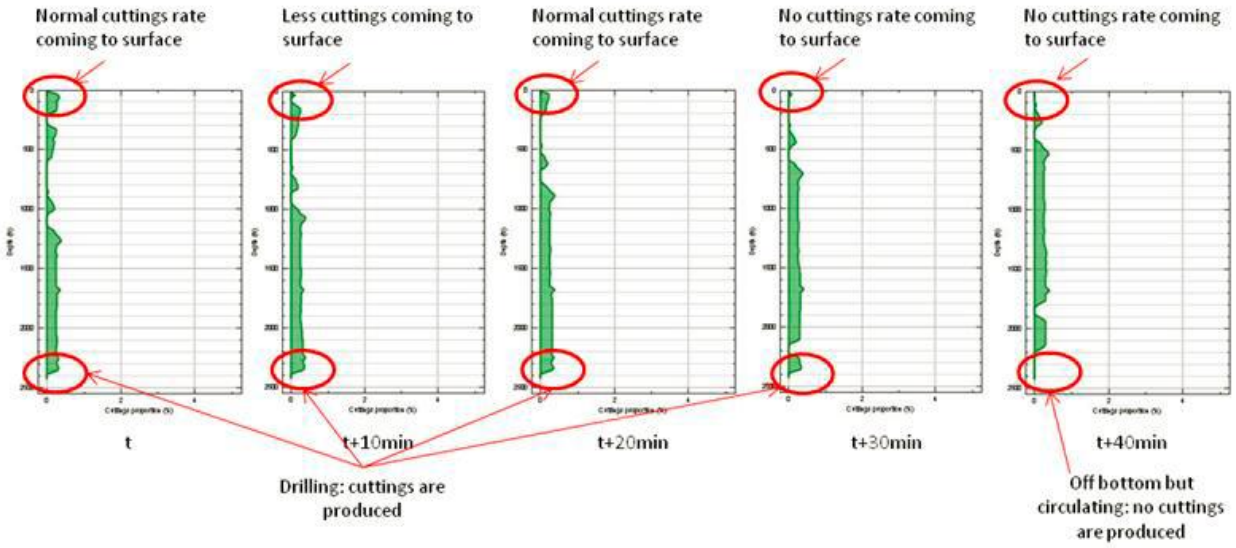

Figure 30: The evolution of the cutting transports proportion along the annulus in function of time by 10 min intervals [24].

Figure 31is the time-based log and shows the expected cuttings flow-rate (green curve) and the relative active volume variation between each mud pump start up. The blue curve is the actual active volume change since the last pump start-up. The rainbow filed regions correspond to different mud losses associated with cuttings removal, the different colors of the rainbow relate to the thickness of the film of the mud which follows the removed cutting removal [21].

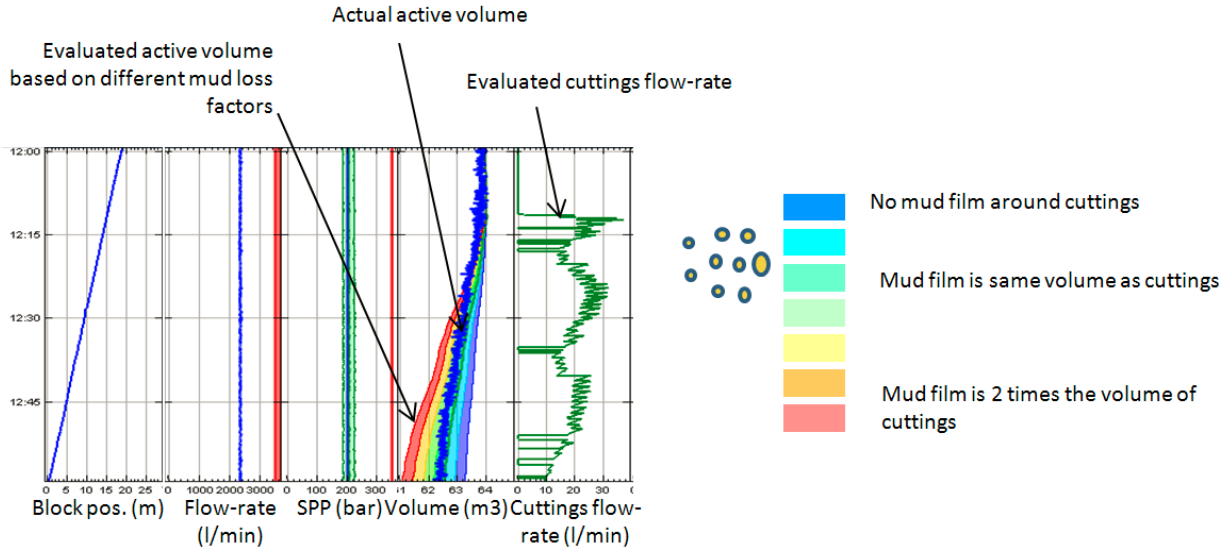

Figure 31: The time based log is showing the expected cutting flow- rate and the relative active volume [21].

Figure 32 shows a case of very poor cuttings transport which was clearly detectable due to the discrepancy between the expected active volume change and the measured value. The track on the far right shows the estimated cuttings flow rate to be separated at the shakers. Track number 3 from the left shows the active volume trend for each stand (corrected for changes in pit configuration). In the volume gradient log, the purple curve represents the measured, while the green curve represents the calculated value. Blue lines are the actual real time measurements while the colored bands in track 3 illustrate the modeled expected volume "loss".

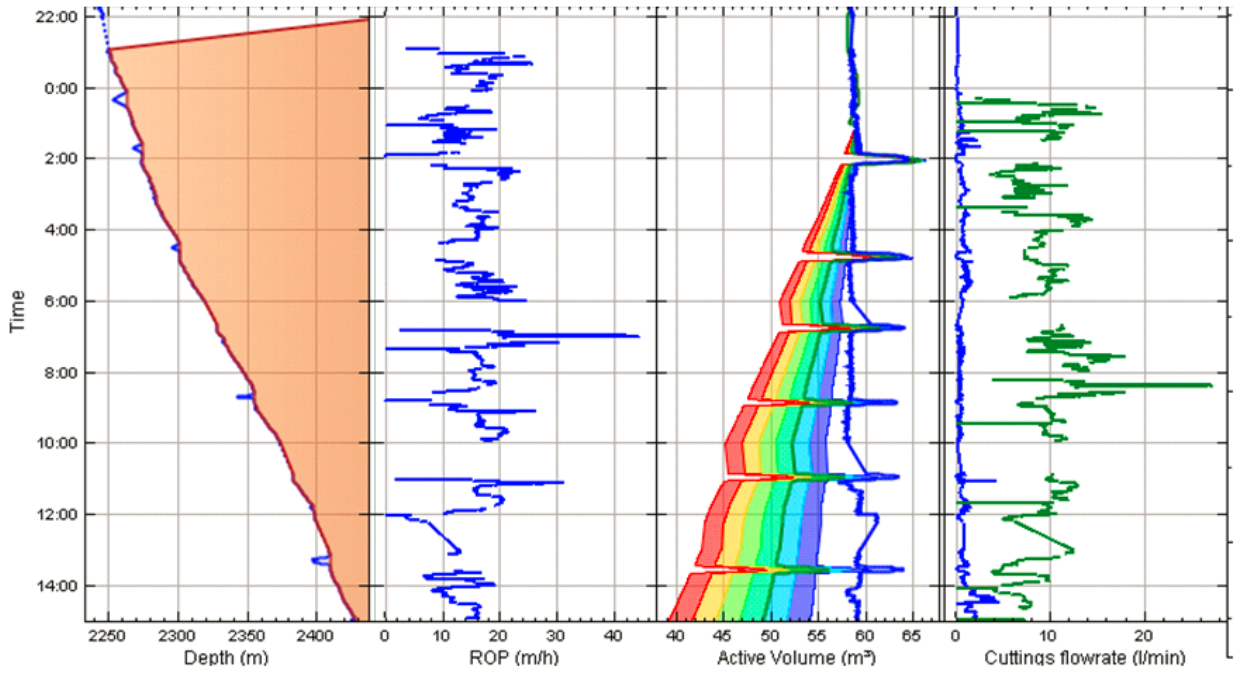

Figure 32: The time base log shows the expected drop in active volume due to cuttings removal [21].

Gain and loss: A difficulty in monitoring gains for kick detection is related to normal variations of the active volume due to changes in flow-rate which can greatly disturb the interpretation of volume changes. When the return flow is established, because a certain amount of mud is accumulated in the surface return system (return channel, shakers, etc.), the flow-rate reduces the level of mud buffered in the return channel drops and an apparent gain is observed in the active volume. The opposite happens when the flow rate increases, more mud begins to accumulate in the surface installations and this is an indication of "loss" [21].

4. DrillScene Monitoring –Case study by this thesis work

This chapter presents the DrillScene advanced real-time monitoring drilling operation for well A and well B. The DrillScene utilized in a pilot test for field North Sea, The pilot was remotely monitored from International Research Institute of Stavanger (IRIS) at Ullandhaug, whereas field A and B monitored by Sekal team.

This study is going to analyze the operation problems and detection that monitored by Drillscene. These analyses will be section by section for both wells. Because of confidentiality, here call the wells as well A and well B.

4.1 Monitoring of Drilling Operation in Well A

4.1.1 Symptoms and Warnings for Section 9 ½", 10 5/8"

4.1.1.1 Increase of the active volume

At 14:37 an increasing of the active volume was observed while performing a flow check. A possible consequence of such an increase in active volume is entering into a well control situation. The level for such situation will depend upon the rate of influx, changing from a small influx that requires no action (in this situation) to handling a possible kick (Figure 33). The well was later found to be static without any actions being taken.

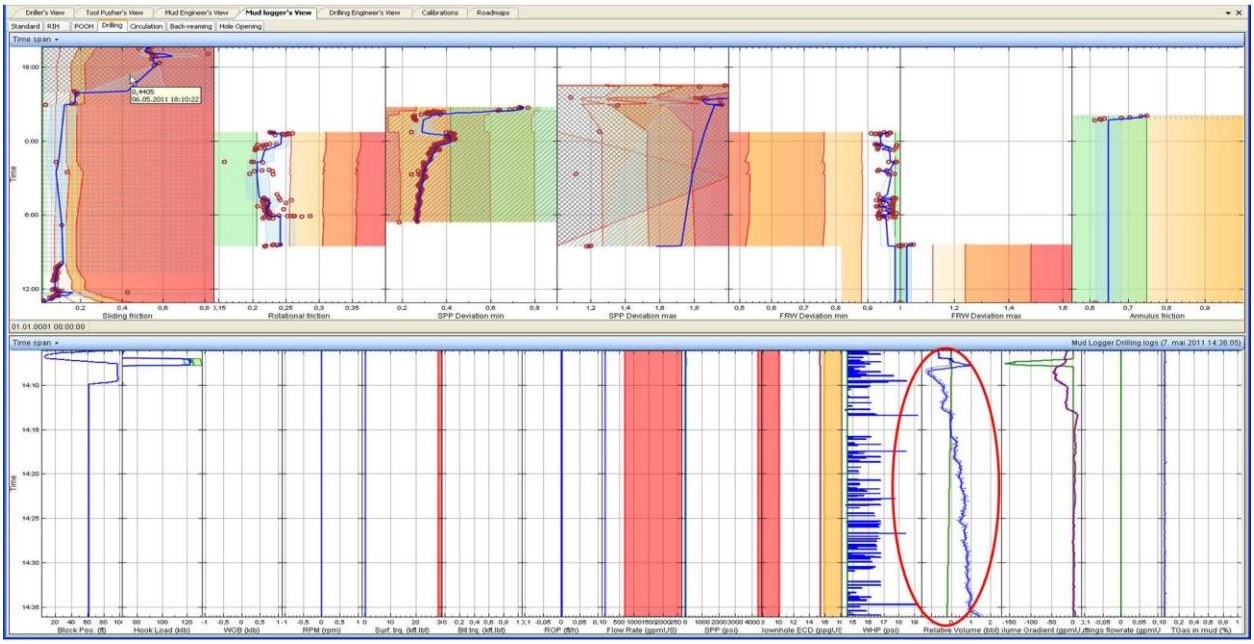

Figure 33: Increasing of active volume while performing flow check.

4.1.1.2 Indication of pack-off tendency

Figure 34 shows, some pack-off tendencies at 13:20, the symptoms for pack-off are an increase in SPP, some spikes in torque, rotational friction increased and a reduction of Free Rotating Weight (FRW) that an increasing of lift-up of the drill -string. At the same time active volume did not decrease, in that case if active volume is not decreased, indicates that the cutting transport was not optimal. The hook load was decreased as well which indicating of pack-off situation. As mentioned before when FRW decreases the drill-string may be lifted up as a piston and therefor the hook load reduces.

Figure 34: Pack-off tendencies, increase in SPP, decrease in hook load, decrease FRW and active volume started to decrease.

4.1.2 Symptoms and Warnings for Section 9 ½", 10 5/8" Side-track

4.1.2.1 Torque spike and reduction of active volume during drilling

From 07:45 while drilling out the cement, torque spike and insufficient reduction in active volume detected. The situation was discussed with the rig and the rig increased the flow rate from 600gpm to 650gpm in order to increase the cutting transport. In such situation with torque spike while drilling out cement and reduction in active volume possible consequence is a stuck pipe situation or a sudden cuttings avalanche Figure 35 below.

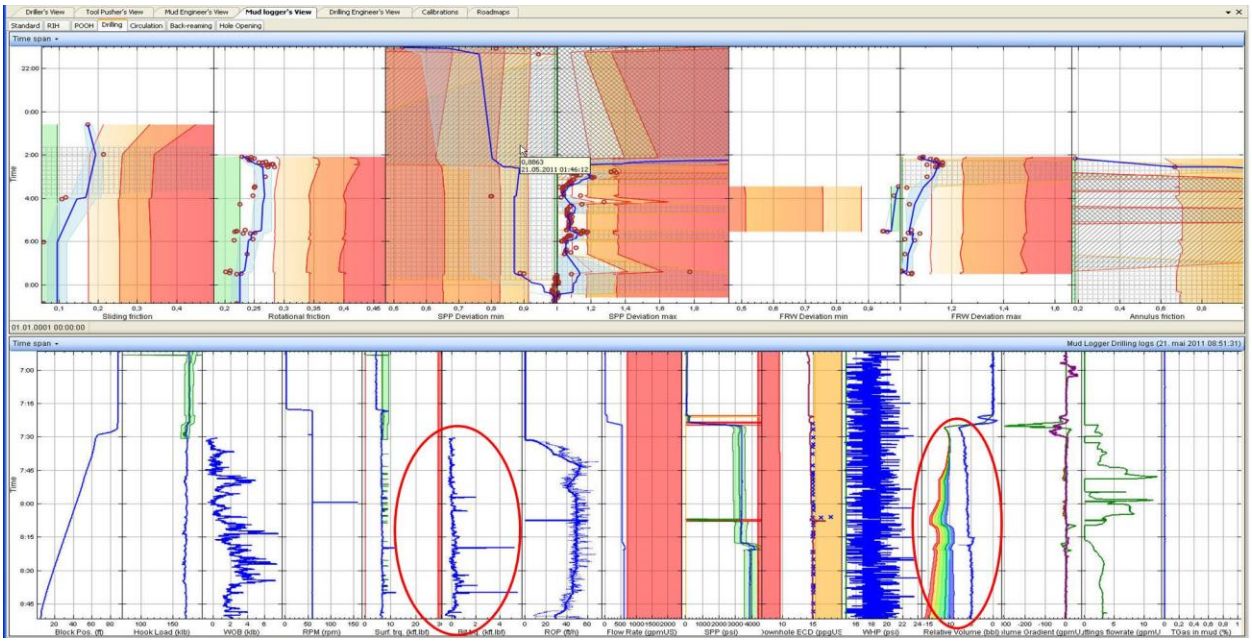

Figure 35: The torque spike and reduction of active volume while drilling out the cement.

4.1.2.2 Pack-off Observation

The FRW shows a drop between 23:15 and 23:30, associated with an unexpectedly low hook load and increasing SPP and some spikes on the surface toque plot. During the hour between 23:00 and 00:00 the rotational friction had increased from 0.18 up to 0.23 over a period of an hour. At 01:00 the data-engineer observed that the rotational friction increased, and the current condition could involve into a pack-off situation. Downhole deterioration at 01:45 was observed that it was a sign for a pack-off situation. At the 02:00 a pack-off situation observed and the result was that the pipe got stuck. From the view of DrillScene, the symptoms leading up to the stuck pipe situation indicated that it was related to hole cleaning (erratic on hook load and surface torque, and increasing of SPP). This was supported by the insufficient cutting transport and the evolution of rotational friction. On the other hand, the PWD did not show any pressure build up, thus leading the rig to suspect that the increased torque was due to the expected gauge of the PDC bit. See Figure 36, Figure 37.

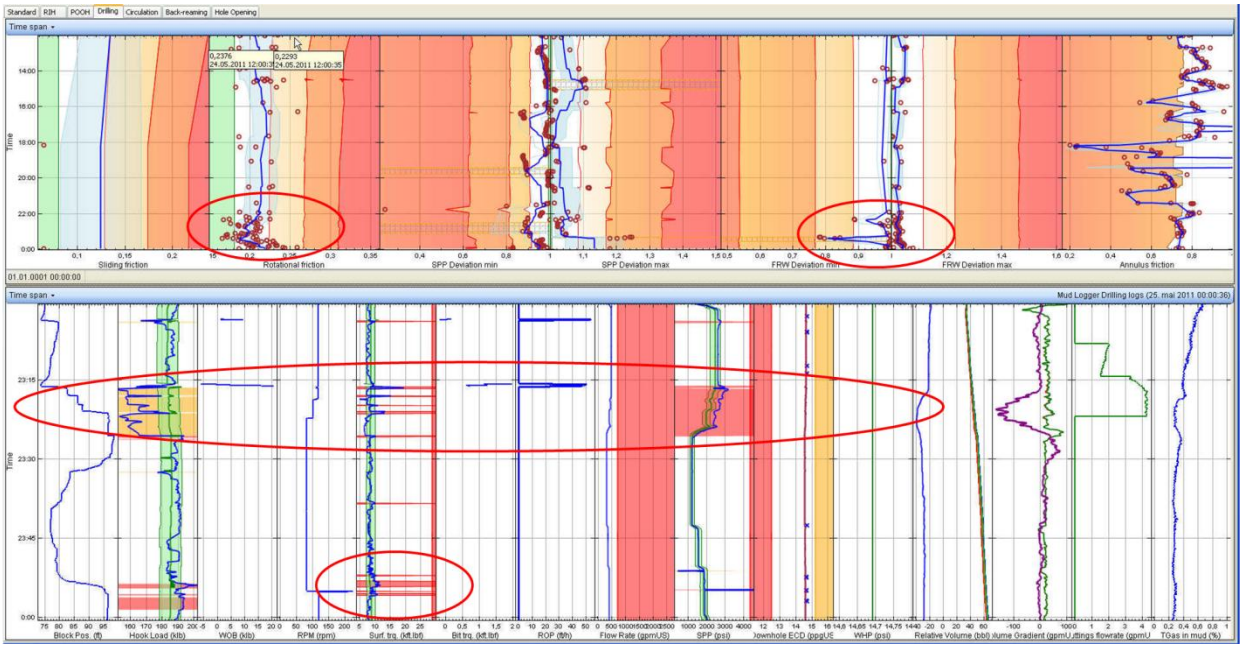

Figure 36: shows the pack-off tendencies between 23:15 and 00:12. The rotational friction increased from 0.18 up to 0.23. SPP is increasing unexpectedly along with an unexpectedly low hook load.

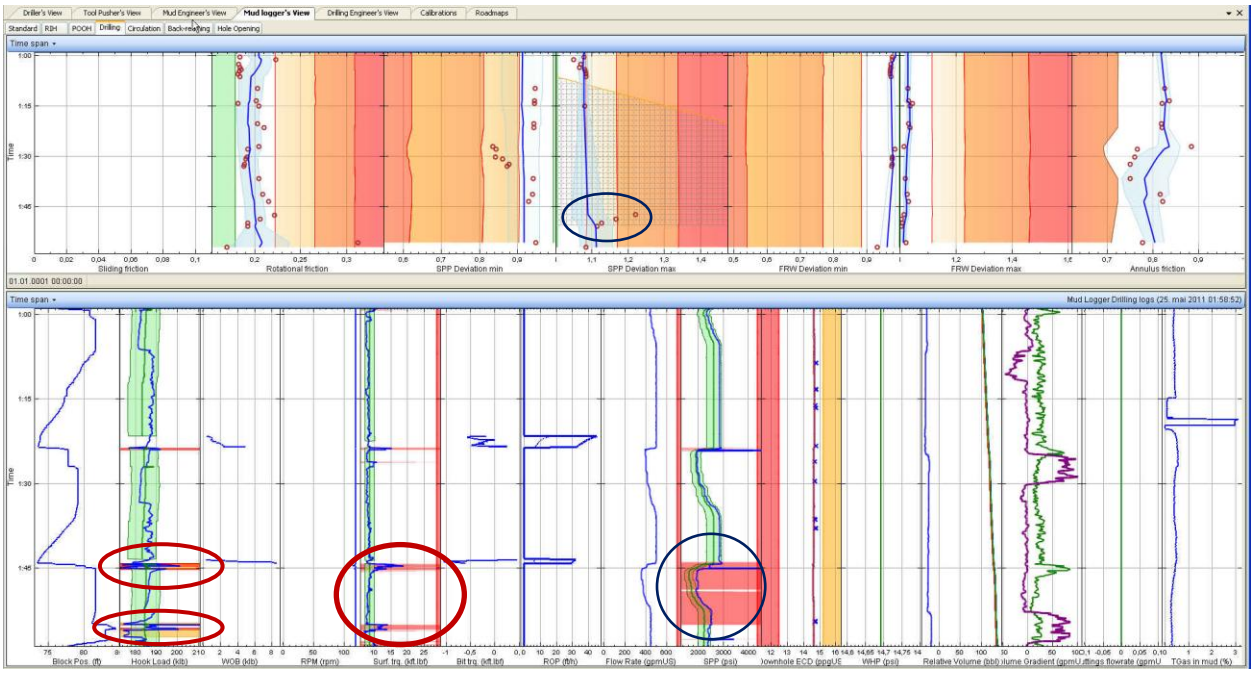

Figure 37: Shows the pack-off that occurred around 02:00

At 03:28, it seems downhole conditions had improved, but increasing in torque and rotational friction appeared when the string moved up and down. At 05:26 as Figure 38 shows, pack-off symptoms were still appearing when the bit was close to the bottom, then the situation informed to the drillers.

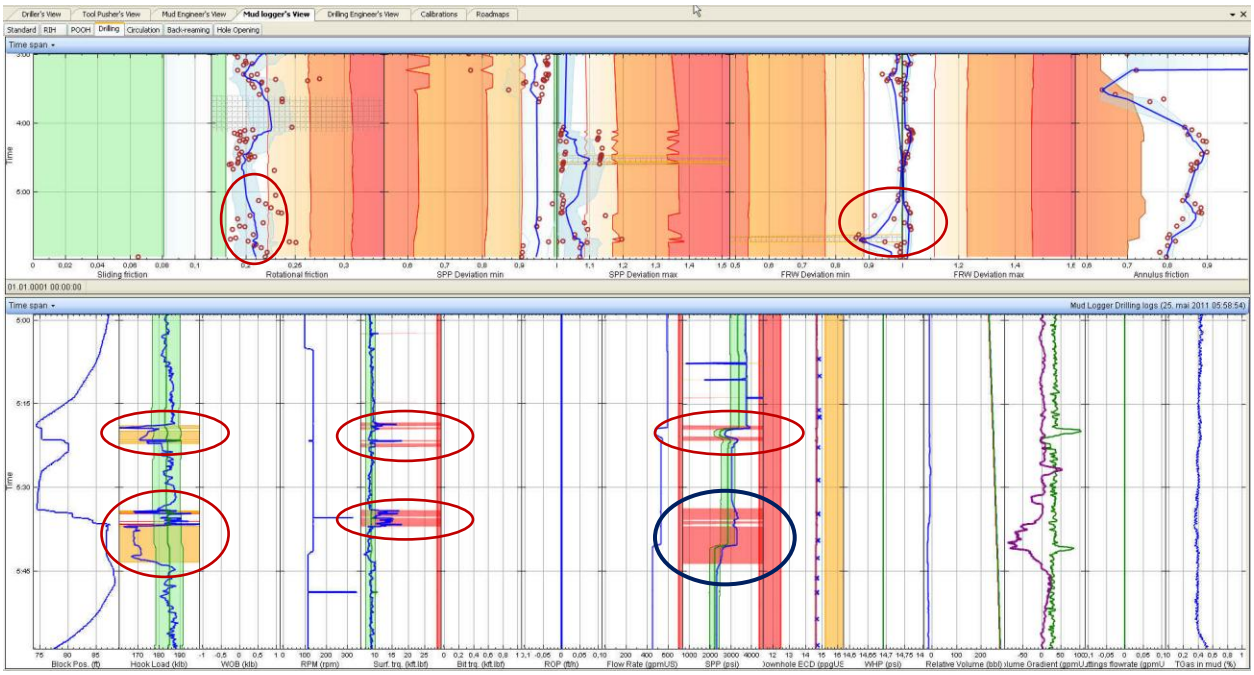

Figure 38: Shows pack-off symptoms when the bit was moved up or down close to the bottom.

The consequences in this case after not performing remedial actions upon the first warning were losing time, approximately 7-8 hours. If the situation were allowed to evolve further, a worst case scenario would be getting completely stuck; losing BHA and side track the section again.

4.1.2.3 Losing mud during POOH and Pack-off during back reaming

Figure 39 and Figure 40 shows two different warnings that were sent by Drillscene symptoms. The first one at 20:47, a warning about losing mud during POOH and the other one was a fracture of formation at 21:57. In the figure 33, one can see an erratic hook load trend, decreasing of the relative volume, erratic on hook load roadmap and an increasing on sliding friction upward.

Figure 40 shows pack-off situation during back reaming that caused the formation fracturing. This fracture was not visible on the calculated ECD plots, since a pack-off situation can cause a rapid pressure build up in the annulus below the obstruction. On the other hand

DrillScene charts show increasing of the rotational friction, SPP and also an erratic trend on the hook load and surface torque.

The actual consequence of this incident was losing fluid to the formation, and the cost associated with the time spent to regain a loss free circulation.

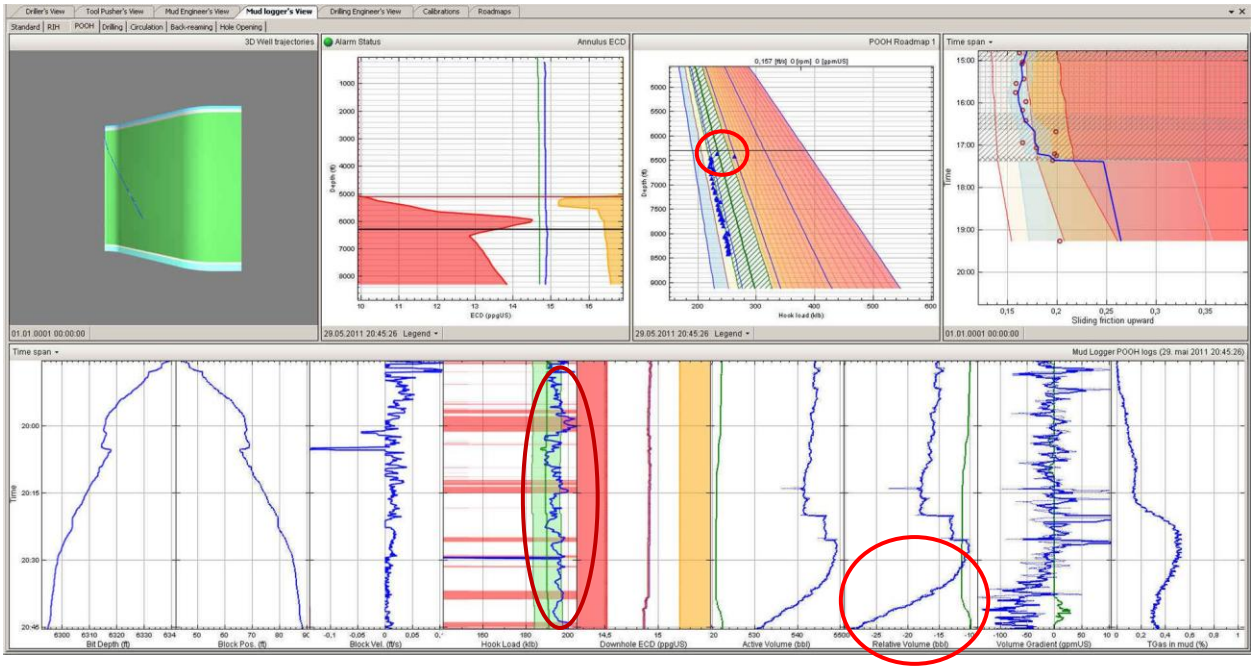

Figure 39: shows the loss situation during POOH

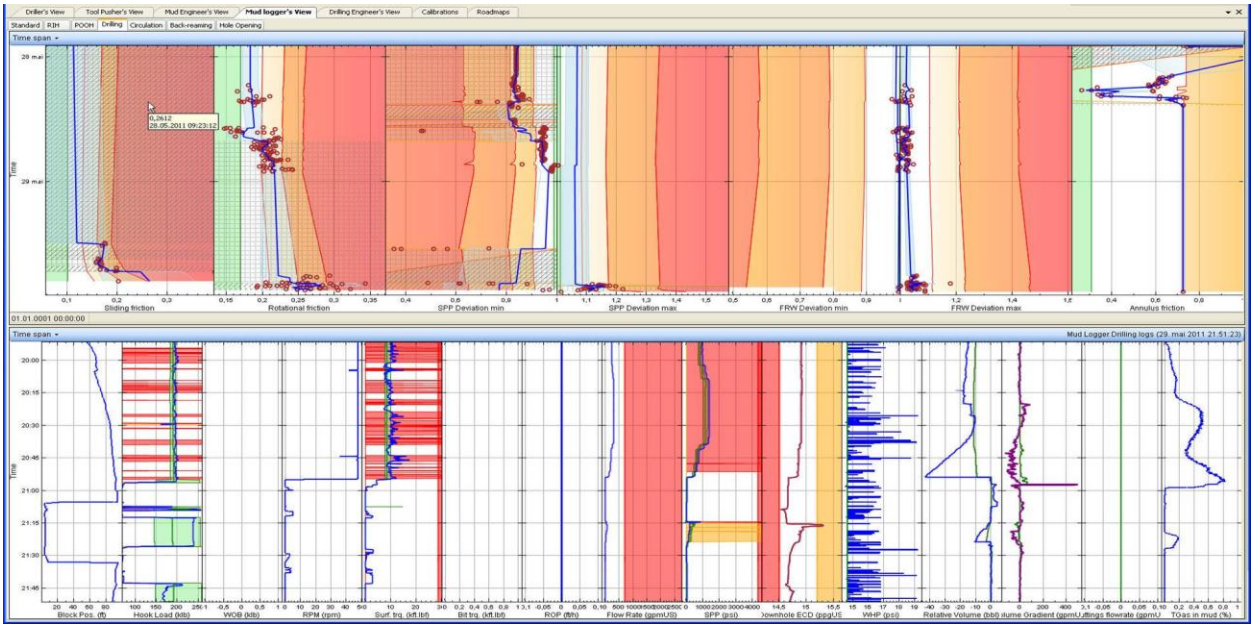

Figure 40: Pack-off situation during back reaming that caused the formation to fracture.

4.1.2.4 Effect on the modeled annulus ECD

During RIH a warning was issued that the tripping velocity caused the downhole ECD to violate the Geo -pressure margin. The situation was discussed with the driller engineer and the rig. The rig decided to reduce the tripping velocity at the beginning of the each stand, thus removing the excessive pressure (Figure 41). The consequence of tripping with a high velocity is possible to weaken the formation at the weakest point in the open hole section, and this can become a problem if mud density will increase at a later time.

Figure 41 Shows that the well started to loose mud after having increased the reaming velocity around at 10:00. This may be a consequence of the well have been exposed to repeatedly excessive pressure while tripping in with a too high velocity. The models indicated that tripping with a too high velocity even far above the casing shoe would cause excessive pressure at depth below the casing shoe.

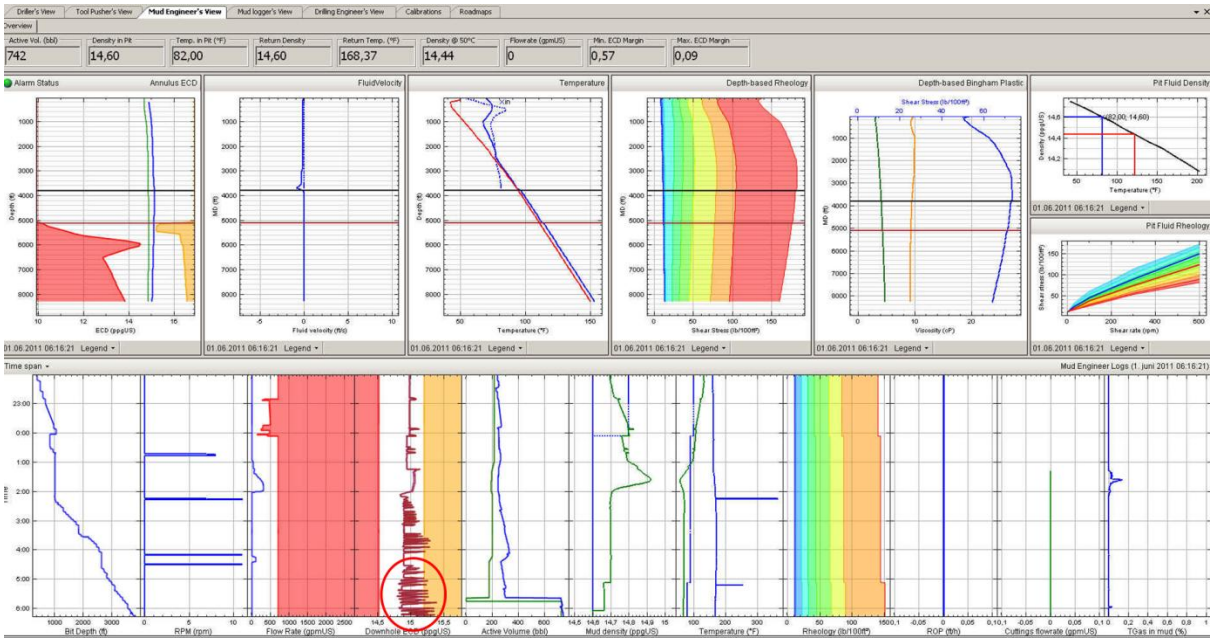

Figure 41: Shows the effect on the ECD when driller decided to increase tripping velocity.

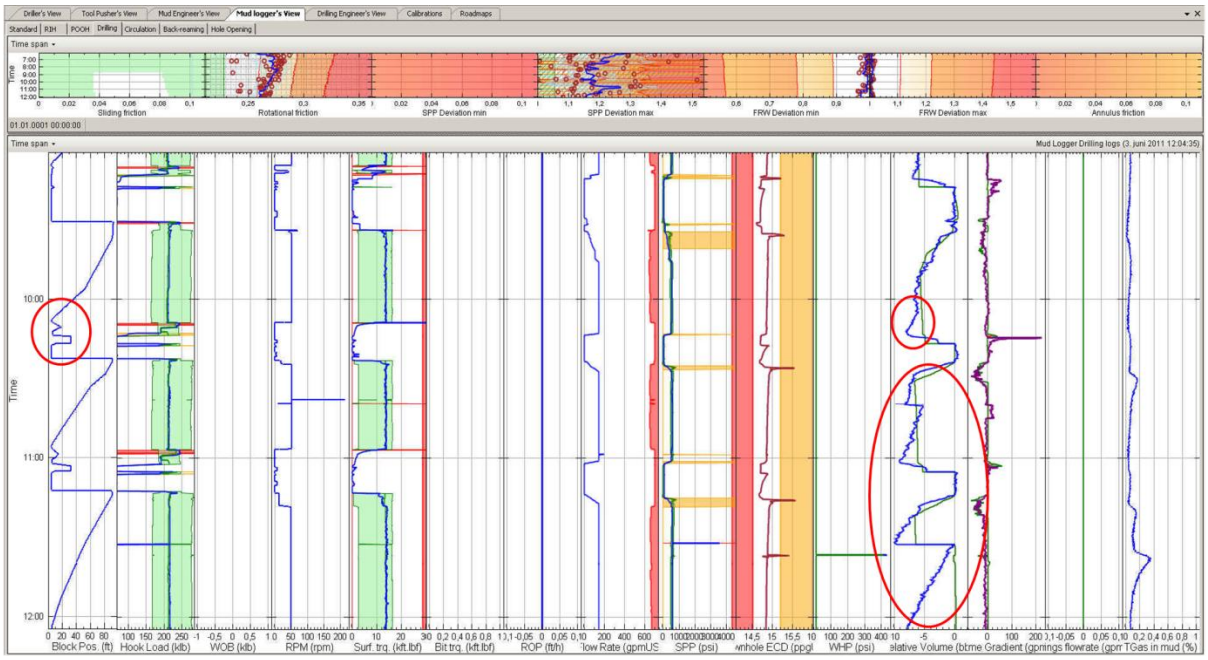

Figure 42: Shows the loss situation after having increased the reaming velocity around 10:00.

4.1.3 Symptoms and Warnings for Section 6 ½" -7 ½"

During this operation several symptoms observed and warnings were sent to the rig. The following warnings observed:

- Warning issued regarding high torque while reaming.
- Warning issued that the active volume was increasing. Such a symptom indicates that there is influx to the well.
- During liner running, the effect on sliding friction from buoyancy effects due to not having configured a float valve in the liner, Figure 43.

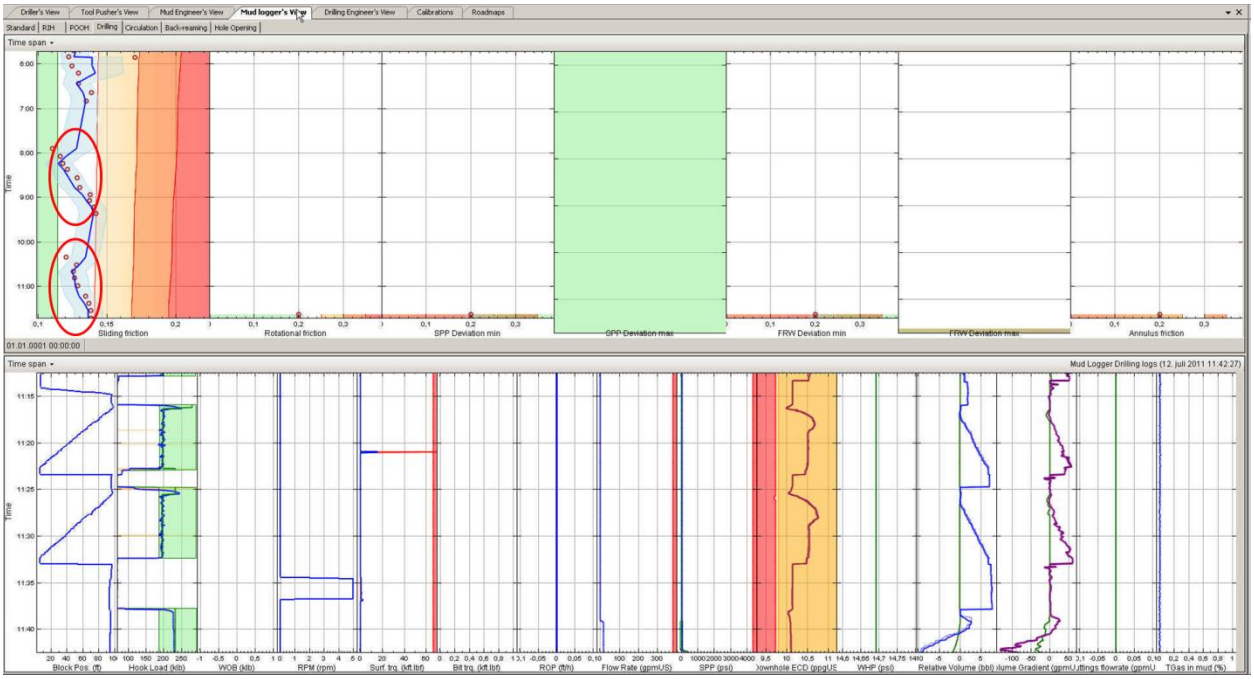

Figure 43: Effect on the sliding friction from buoyancy effects.

4.2 Monitoring of Drilling Operation in Well B

4.2.1 Symptoms and Warning for section 12 ¼

4.2.1.1 Indication of pack-off tendency

Figure 44 shows the result from the chosen drilling sequence. At 15:30 an increase in SPP deviation and the reduced FRW deviation was observed. During the drilling, active volume did not reduce as expected, when accounting for cuttings removal, active volume increased from the expected area and this indicated the poor cutting transport. Hook load was decreased as well which are indication of pack-off situation. Therefor a follow up warning email was sent.

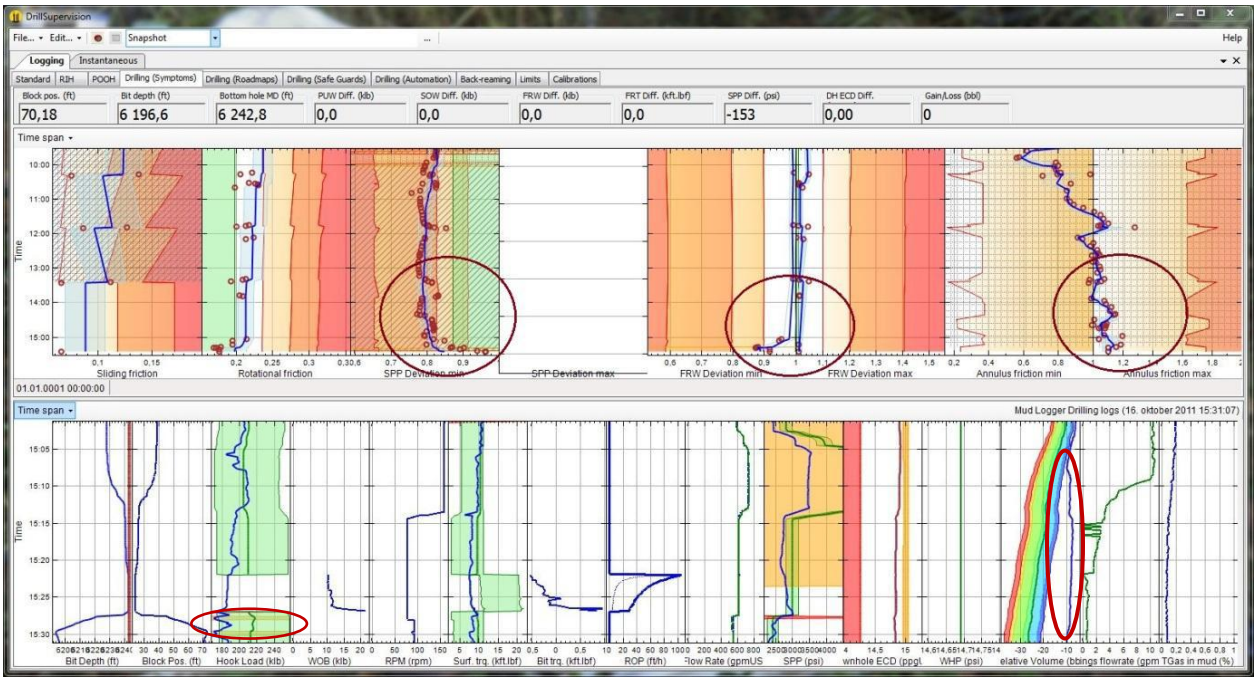

Figure 44: Increase in SPP deviation and increased active volume

Another pack-off situation started from 03:04, the following symptoms were observed: SPP increased, rotational decreased, and hook load lower than the expected value, FRW decreased which gave warning signs that the downhole conditions worsen. There was a spike in surface torque of 23klb and slack-off weight reduced to 100klb Figure 45.

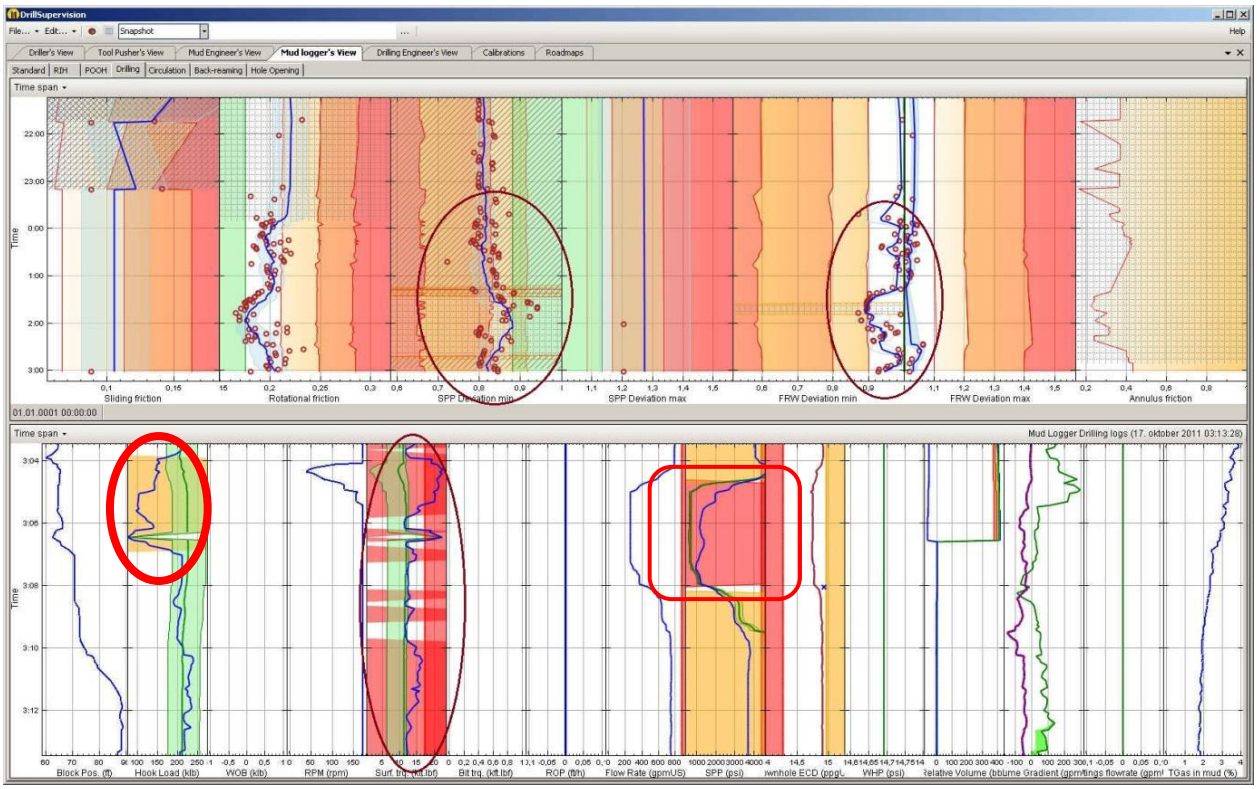

Figure 45: Increased in SPP, decreased FRW and low Hook load trend.

4.2.1.2 Pick-up weight and high torque

Torque spikes were observed while reaming down and back-reaming. Also the high sliding friction points corresponding to the pick-up weight. Also at 05:00, the corresponding increase in rotational friction and in SPP deviation was observed. This was an indication that something is packing around the BHA, causing the high torque and blocking flow which caused the SPP increase for a short time.

High off-bottom torque observed as compared to what it should be after drilling the stand up to 11,299ft MD result in high rotational friction, an indication of poor hole cleaning. At the same time, SPP was on the slightly decreasing trend. Pick up weight was high also during the friction test. PWD (pressure while drilling) values also slightly decreased. All these are an indication of possible hole collapse issue. It was an assumption that some cavings observation, but after discussion with data engineer result was no cavings and if there are, these were very small. See Figure 46.

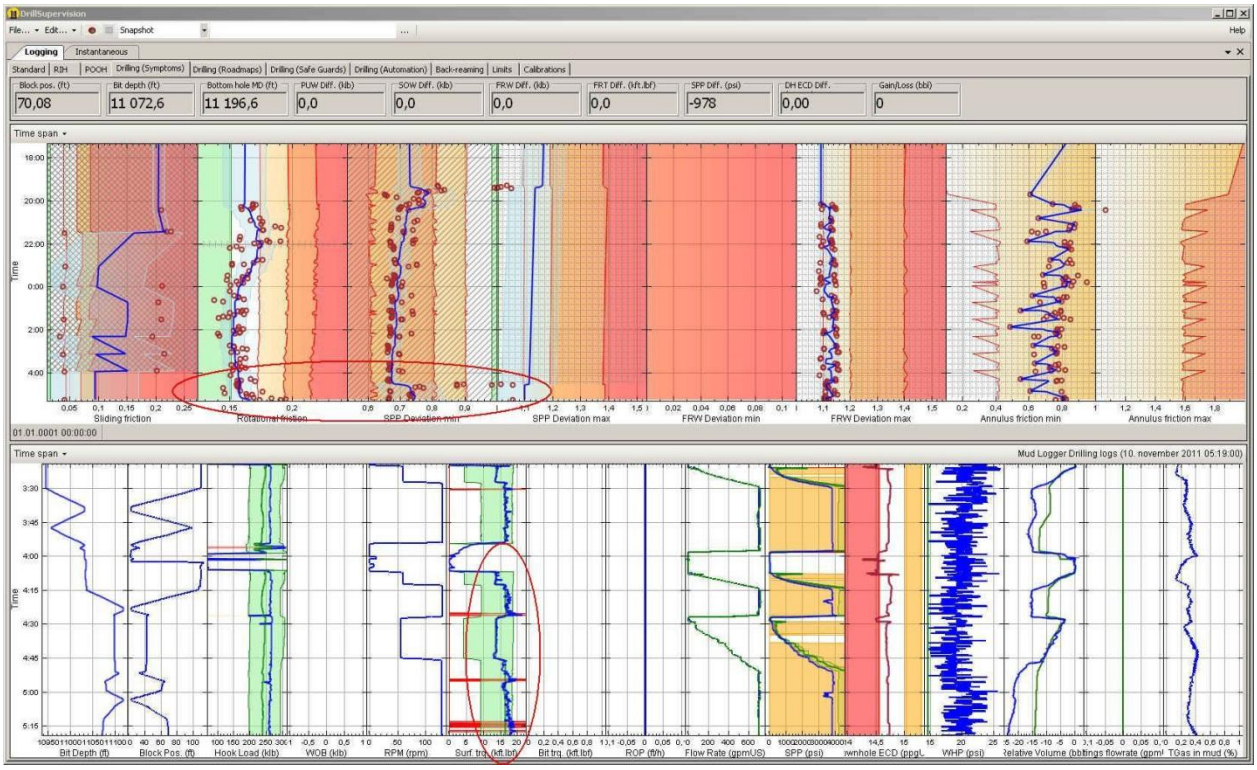

Figure 46: Increase trend of Rotational friction, SPP deviation and torque spikes.

4.2.1.3 High off-bottom torque during Back –Reaming

Figure 47and Figure 48 are showing the symptoms during back-reaming. High torque started from 09:15 during back reaming of depth of the 11,900 ft MD corresponding to increase in Rotational and Sliding Friction. Also decrease trend in relative volume shows loss of mud as well.

While back-reaming, a slowly increasing trend in Rotational Friction, and PWD values was observed around 19:22. The match between the calculated and measured surface torque is not good and annulus friction increased in maximum areas. All these were signs of something packing up while pulling. After discussing with data engineer and the rig the result was to pull slowly.

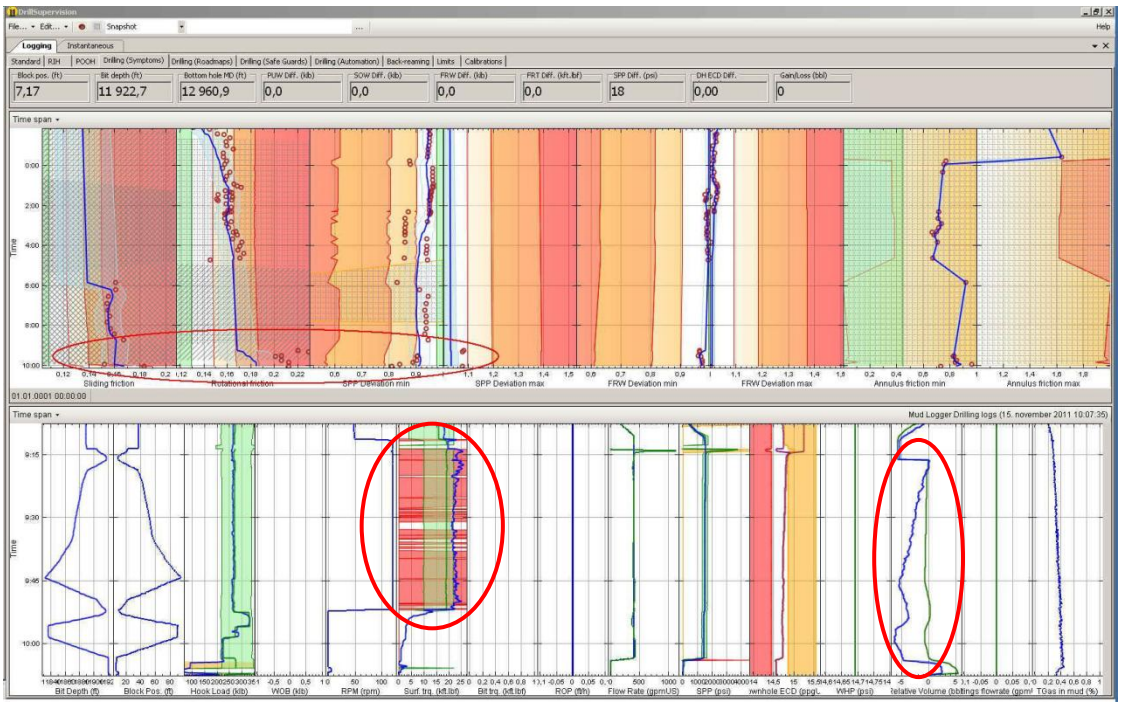

Figure 47: High surface torque during back-reaming.

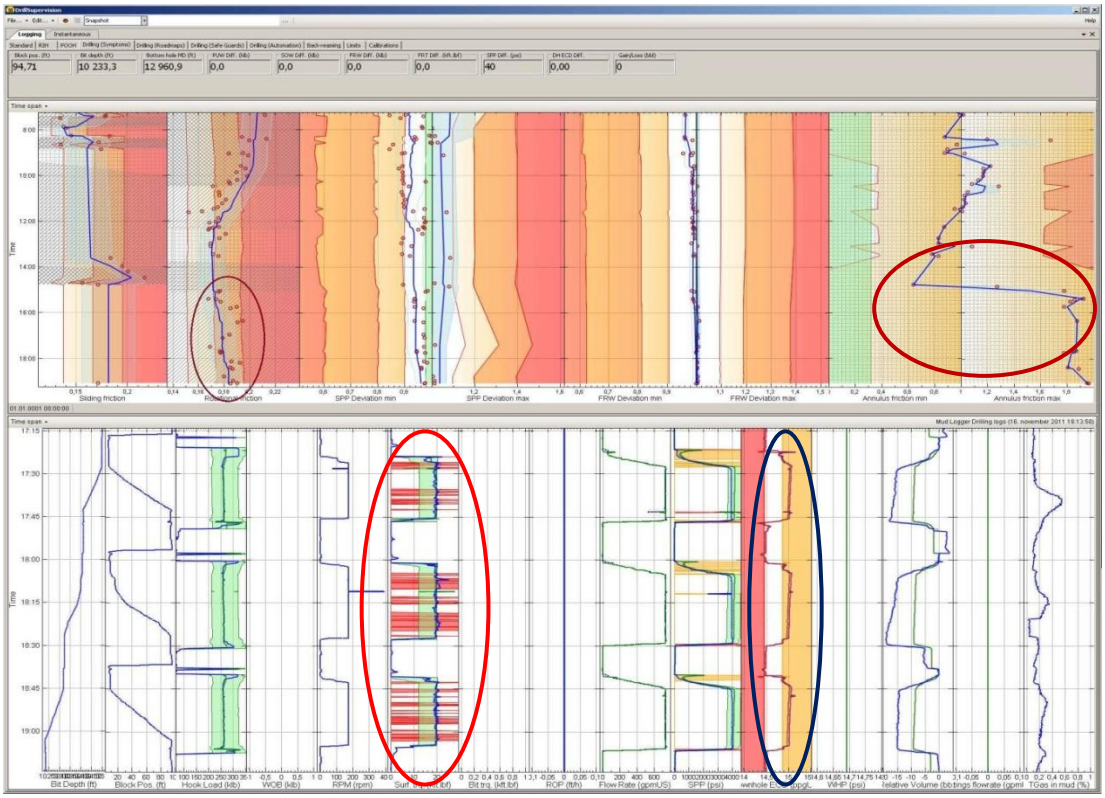

Figure 48: Increase in Rotational Friction, Annulus Friction and violation of fracture gradient.

4.2.1.4 Violation of fracture pressure during POOH

Around 07:55, it was an observation of fracture pressure that shows it being to violate at the shoe during circulation. Small losses were also observed. A warning was sent to the rig, the action was to reduce flow rate, then the losses stopped Figure 49.

Around 08:11, a total volume (losses) started accruing when the pumps were started. The losses were in order of 125bbl/hr according to the data logger. The pump rate was reduced as a consequence of the losses, and the losses stopped. An increase in active volume -too rapid and too heavy was observed. The rig informed that they observed gain on the bell nipple. Action was to shut in the well immediately.

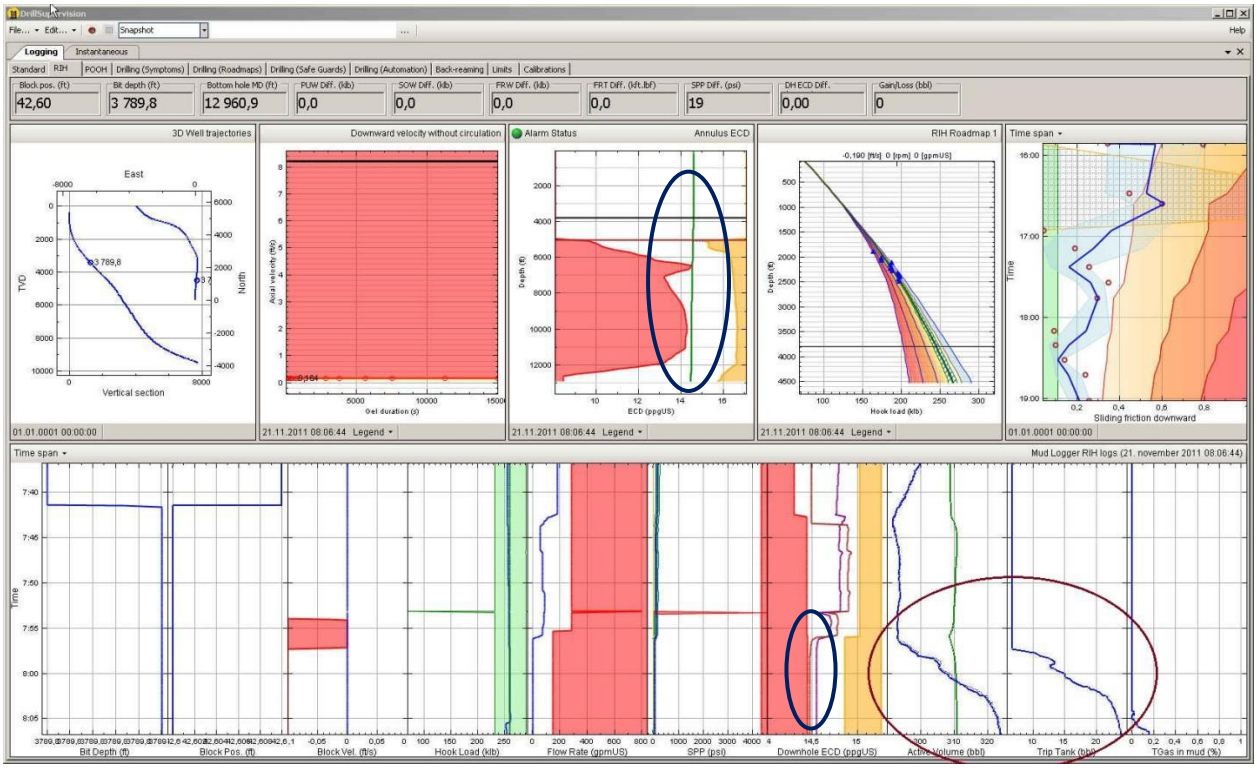

Figure 49: Violation of fracture gradient and Gain in trip tank.

4.2.2 Symptoms and Warning for section 8 ½ -9 ½

4.2.2.1 Loss to formation during RIH

At 16:45 when the bit was at the depth of 10045 ft MD, some losses were observed with the rate of 350 gpm. The first action was to reduce flow rate, so the loss decreased to 260 gpm. The flow rate reduced to 90 gpm than loss was controlled. An attempt was made to cure the loss by adding LCM (Lost Circulation Material) and establishing loss free circulation which was achieved at a flow rate of 510 gpm. Figure 48 shows the loss and ballooning effect after curing.

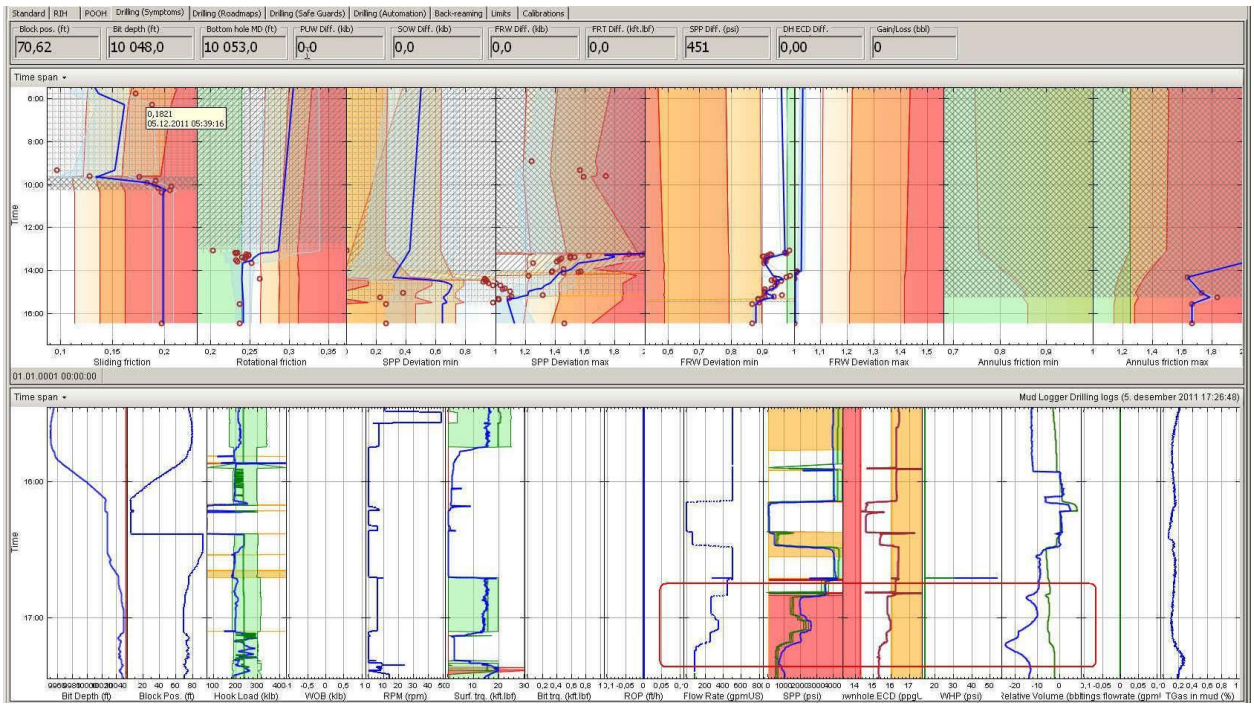

Figure 50: Ballooning effect after controlling loss below casing window.

Since ECD was very close to fracture gradient, limited volume of mud loosed to the formation. This happened when the BHA was passing the casing window.

After drilling one stand and during a survey and sending downlink, high values in surface torque, SPP and some spikes in surface torque and hook load was observed. At 00:50 sudden loss was experienced and the decision was made to pull out into casing and establish loss free circulation Figure 50.

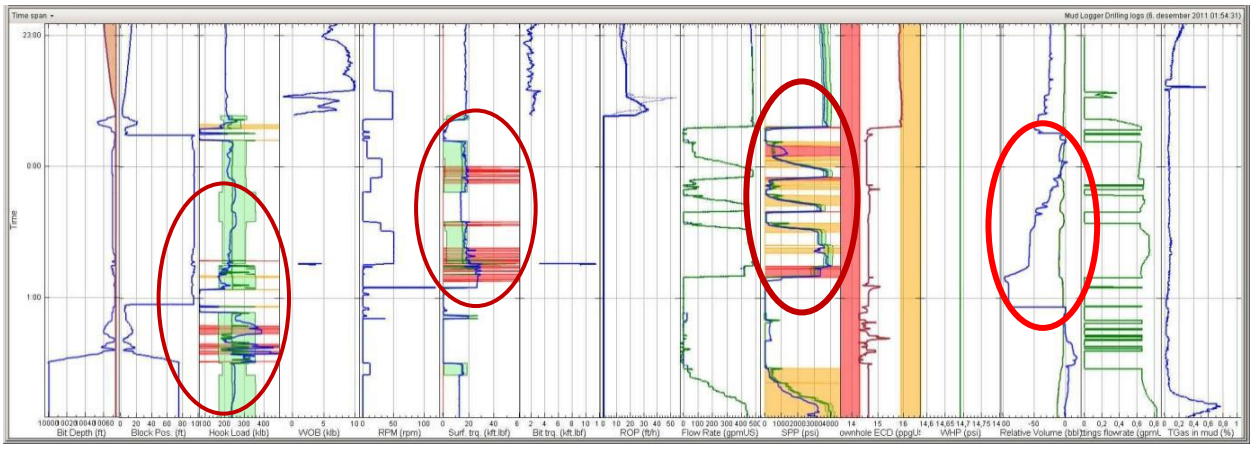

Figure 51: High values of surface torque, SPP with overpulls and loss.

Three attempts were made to pull out which two of them were failed due to over pull of string. The overpulls could be related to passing Geopilot through the window see Figure 51.

4.2.2.2 Pack-off while reaming down and loss to the formation

At 03:30, the hook load decreased and sudden SPP increased with reduced flow rate which this is an indication of the pack-off. Loss of 30bbl also observed. Annulus friction was increased up to maximum part.

During drilling the ECD and PWD values were very close to the fracture gradient it was because of the hard formation, Figure 52.

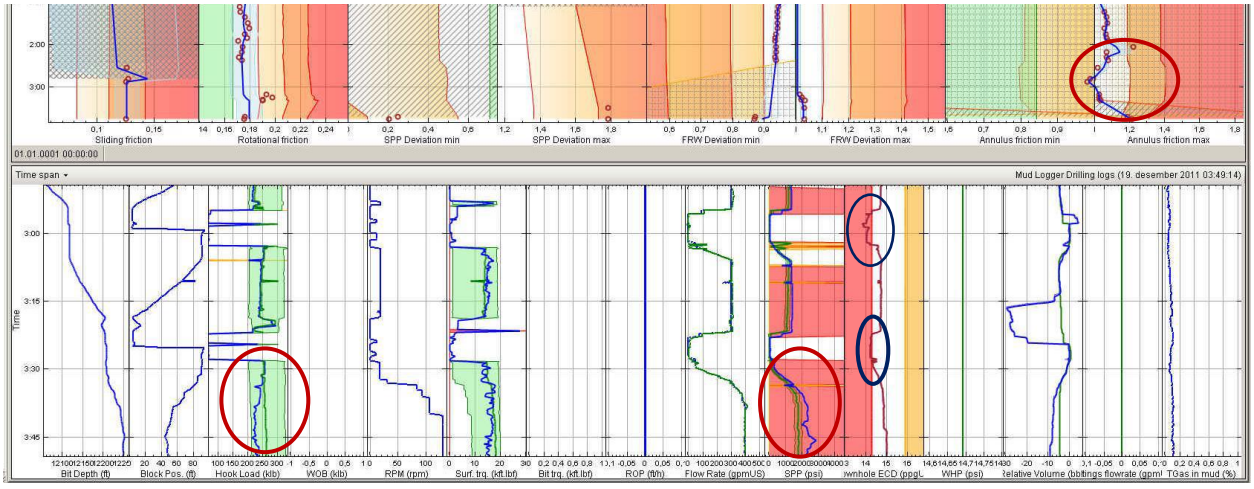

Figure 52: Early indication of possible pack-off.

At 23:00 loss to formation observed due to decreasing relative volume and annulus friction at the minimum. Initial loss was 100bbl/hr which reduced to 65 bbl/hr. LCM added to cure the loss (40 bbl) Figure 53. Loss flow was reduced by decreasing the flow rate and adding LCM to circulation system. Increase of the flow caused to start and loose more mud to formation.

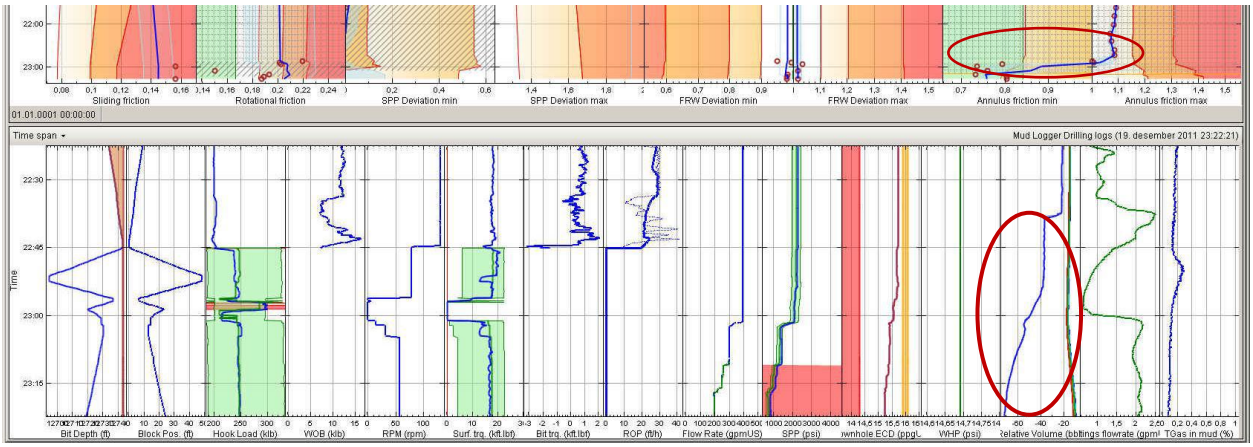

Figure 53: Losing to formation due to decreasing in relative volume.

4.2.3 Symptoms and Warning for drilling cement section 6 ½ - 7 ¼

Cement plug was successfully drilled, during reaming the cement plug high surface torque was observed. During POOH several over-pulls versus the modeled hook load was observed see Figure 54 below.

Figure 54: several over-pull during POOH

4.2.3.1 Clean out and drilling section

During RIH when the bit was passing the depth of the 11700 ft MD, sliding friction increased significantly. Circulation started to clean the possible cement particle from previous cement job see figure 55.

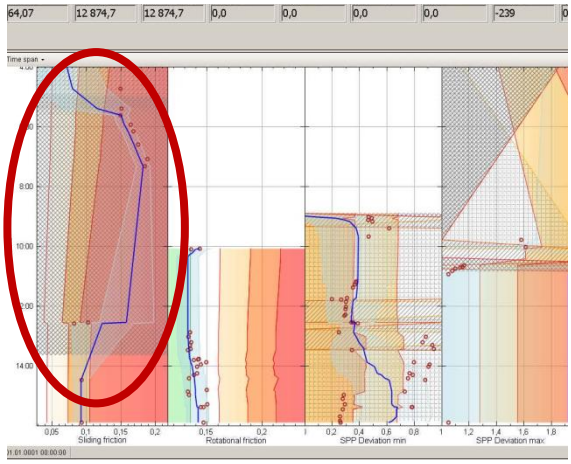

Figure 55: Increase in sliding friction.

Figure 56 shows loss during drilling around 04:00. The Annulus Friction is evolved from the difference between measured PWD and the modeled ECD at the bit. Drillscene's dynamically modeled ECD considers the cuttings proportion in annulus, but when the cuttings accumulate around the BHA then the PWD increases more than the modeled ECD. During normal drilling operations these accumulated cuttings moved above the BHA whenever reaming and circulating off-bottom after each stand, causing the zigzag pattern in the Annulus Friction.

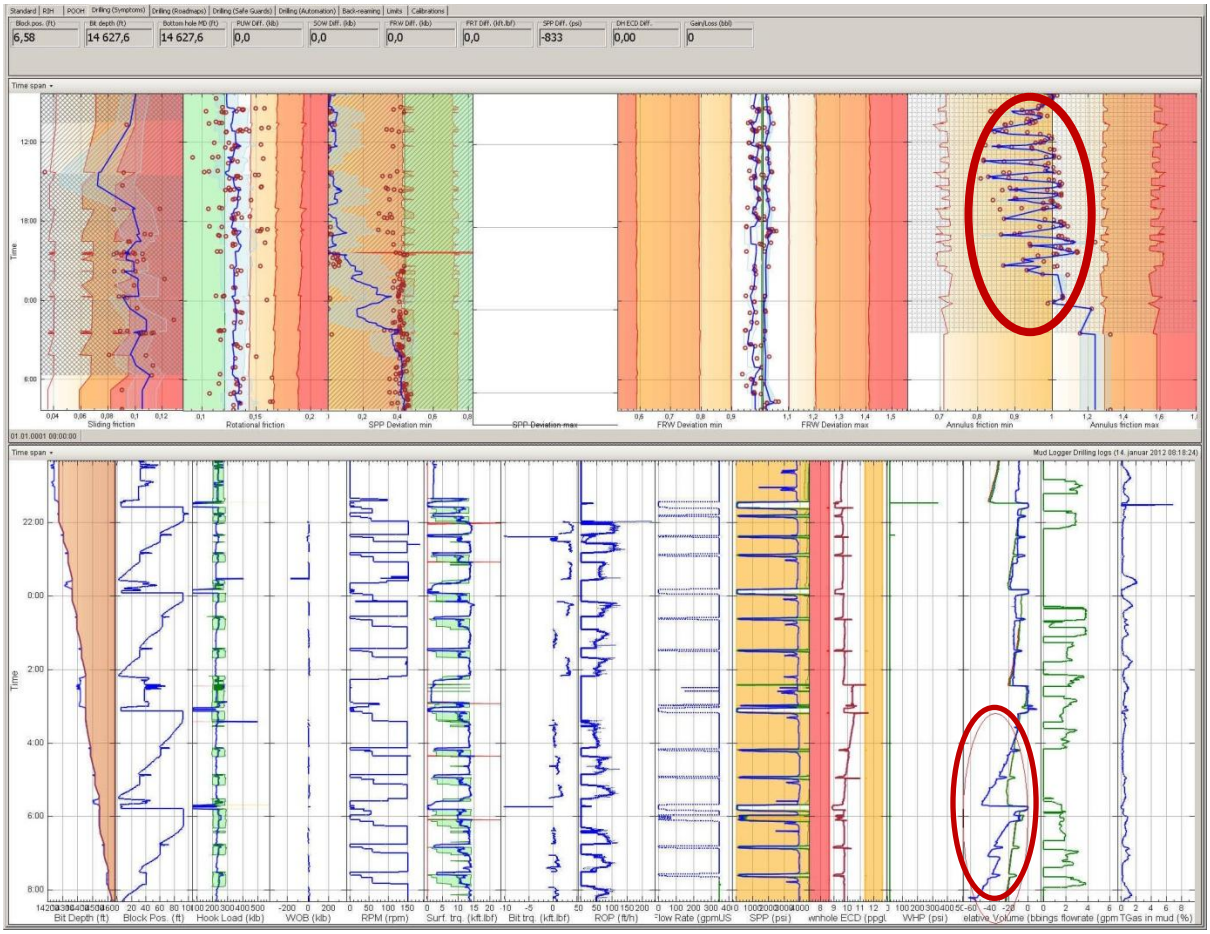

Figure 56: Losses and Annulus Friction

4.2.3.2 Observation Loss and Gas in Reservoir

Small loss was observed due to decreasing of relative volume the reason for this problem after discussing with data engineer was that some of the fine mesh screens were removed from the shakers to recirculate LCM and finer particles back into the well to provide better fill in case of small fractures.

The ECD plot was very close to the fracture gradient prognosis but the connection gas was still increasing up to 8.5%. To avoid having more gas in the mud while drilling the reservoir section, the mud weight and subsequently the ESD/ECD was increased. At the same time the more LCM material was added to the mud in order to reduce or prevent mud losses to the formation according to mud logger.

Since the reservoir section was horizontal, off bottom circulation was necessary to bring the cutting to the surface. By keeping the ECD higher than the fracture gradient prognosis there was an increasing risk of loss circulation in the case of facing natural fractures. So the result was to set TD earlier than planned.

LCM screen-out started after reaching TD, the apparent mud loss was due to removal of LCM material with finer mesh screen at the shakers and no mud was lost to the formation see Figure 57.

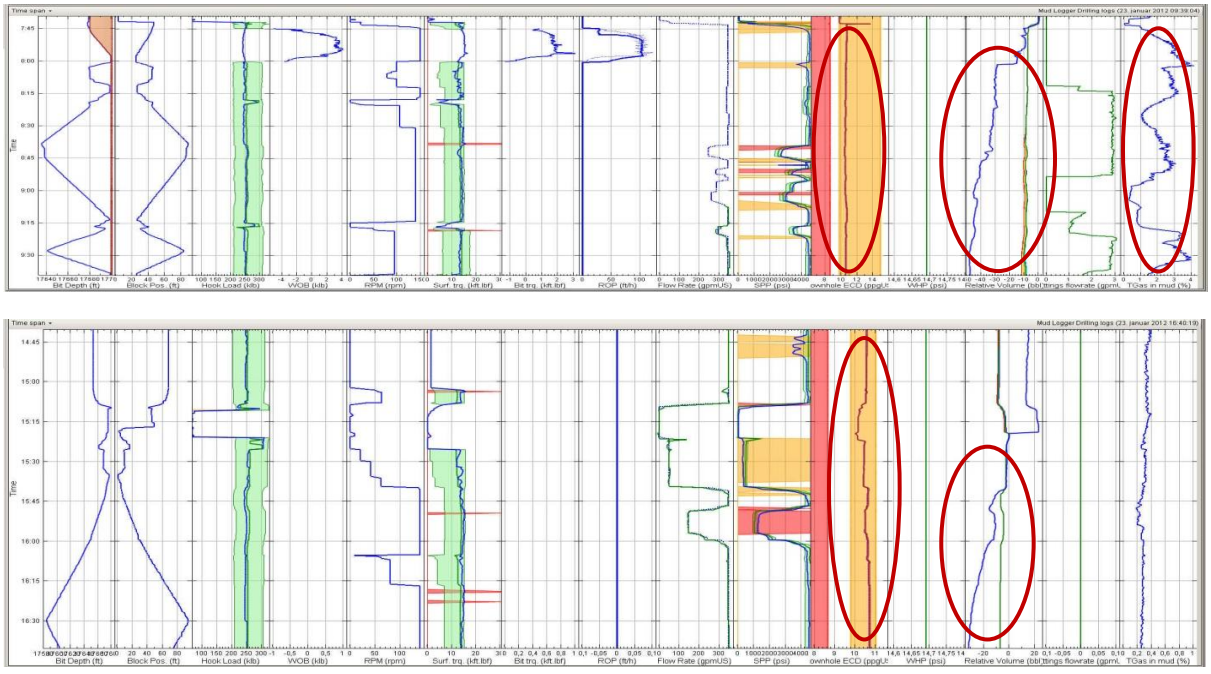

Figure 57: LCM screen out and ECD higher than fracture gradient

During pulling of hole while reaming upward started the LCM was removed from the well. To avoid potential influx while tripping out, the rig increased mud weight to 10.3 ppg. In this case hook load was increased when passing through the casing shoe, which was normal.

4.2.3.3 Set-down weight while running production liner

When the liner running operation started into the open hole, the Sliding Friction started to increase rapidly that affected the hook load which approached the lowest limit of the DrillScene model (Set-down weight).

The problem was that the string was buckling during slack-off and the liner had to be rotated and circulated to reach bottom, Figure 58.

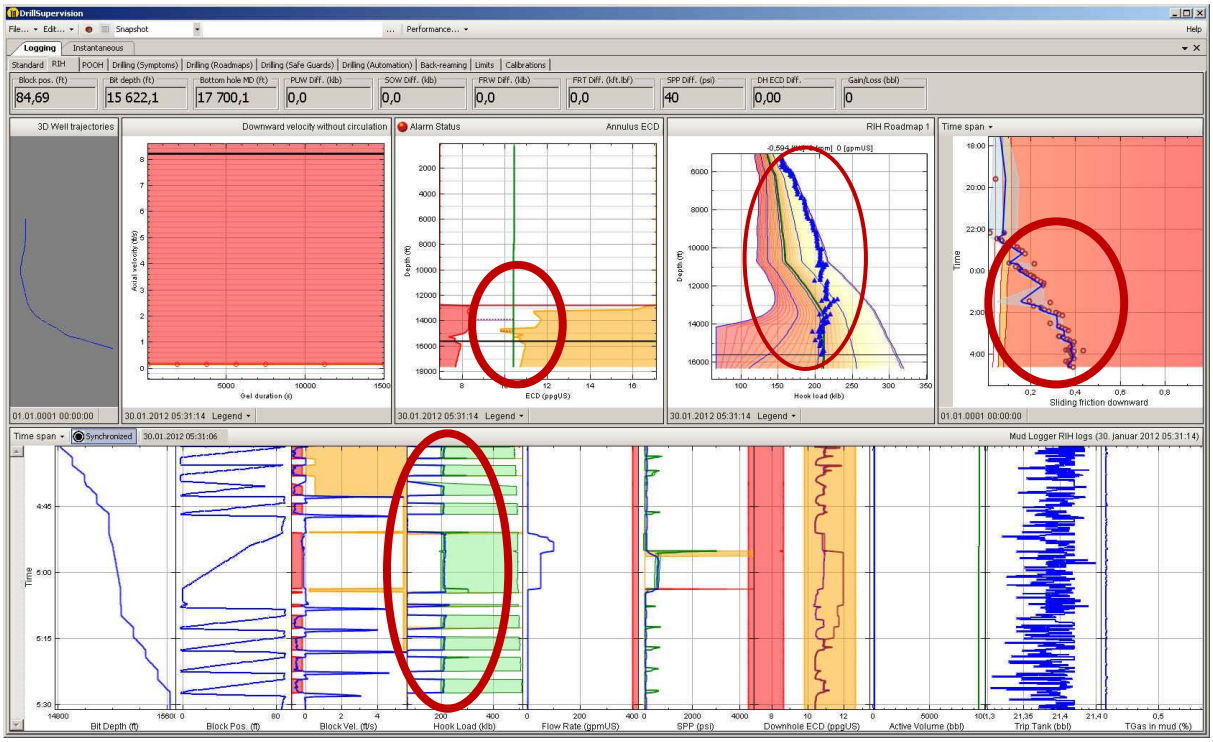

Figure 58: Increasing in Sliding Friction with low Hook Load.

5. Summary and recommendation

Summary

During drilling operation, downhole conditions can be changed and lead to unexpected situation which can result in loosing time and cost. In traditional drilling, due to non-productive time (NPT), the well incidents such as kick, stuck pipe, pack-off, mud loss, well collapse and equipment failures and thus cost of drilling is unavoidable.

Real-time monitoring is a newly development drilling automation system that monitors downhole conditions to avoid abnormal drilling situations by pre-emptive actions. This technology reduces non-productive time (NPT) that causes by drilling incidents.

The system analyzes the following signals continuously: sliding and rotational friction, downhole and pump pressure, free rotating weight deviations, relative volume, pit volume, hook load, flow rate, rate of penetration (ROP).

The method exists in recording and measuring pick-up weight, slack off, free-rotating torque while drilling. This software has the advantage of simplicity and can be used by any drilling engineer to detect pack off situation by using symptoms such as friction plots (sliding friction, rotational friction, annulus friction), hook load, surface torque. By DrillScene one can observe poor hole cleaning by relative volumes, cuttings flow rate.

The DrillScene system is a powerful tool in which based on physical models detects various symptoms related to downhole conditions during drilling operation.

Based on the two case studies (i.e in Chapter 4) and case studies done by IRIS (i.e in Chapter 3), it has been found out that the DrillScene Advanced Monitoring Services is a powerful tool to detect changes in the downhole conditions during drilling operation. Such changes can represent symptoms of deteriorating conditions that are likely to evolve if no actions are taken. The symptoms can thus be used as decision support for performing remedial actions or to give an overview of the status of the drilling process.

Recommendations

From the monitoring of real time data, we can observe that some warning signals are not really an indication of downhole problems and they could be due to false sensor readings. Engineers who are monitoring the real time data with Drillscene at onshore/offshore drilling operation center should have:

- Knowledge /practical experience
- Knowledge of the drilling process very well
- Need to get proper training in IRIS training center in order to have a good understanding of the software and interpretation techniques.

6. References

1. Aadnøy B.S (2003) Journal of Petroleum Science and Engineering 38(2003) 79-82.
2. Bernts. Aadnøy: "Modern Well Design", Rogaland University Center, Stavanger, Norway
3. C.A. Johancsik, D.B. Friesen, Rapier Dawson: "Torque and Drag in Directional wells-Prediction and Measurment", SPE Exxon Production Research Co., June 1984.
4. Johancsick C.A., Friesen, D.B. Dawson,R(1984). "Torque and Drag in directional Wells-Prediction and measurement", Journal of Petroleum technology, June 1984.
5. Terje Tveitdal, 2011 "Torque & drag analyses of North Sea Wells using new 3D model", Master thesis.
6. B.S.Aadnøy:"Mechanics of Drilling", University of Stavanger, 2006.
7. S.L.Sah : "Encyclopaedia of Petroleum Science and Engineering, published 2004.
8. Mustafa Versan Kok, Tolga Alikaya: "Effect of Polymers on the Rheological Properties of KCL/Polymer Type drilling Fluids" , Department of Petroleum and Natural Gas Engineering Middle East Technical University Ankara, Turkey, Energy Sources, 27:405-415, 2005
9. Ekwere J. Peters, Martin E. Chenevert, Chunhal Zhang: "A Model for Predicting the Density of Oil-Based Muds at High Pressures and Temperatures", Journal Paper, June 1990. Page 141-148.
10. Øistein Glasø,:"Generalized Pressure-Volume-Temperature Correlations", Paper 8016-PA, Journal of Petroleum Technology, Volume 32, Number 5, May 1980, pp 785-795.
11. Sorelle R., R.A. Jardiolin, P. Buckley, J.R. Barrios, 1982: "Mathematical Field Model Predicts Downhole Density Changes in Static Drilling Fluids", Paper 11118-MS presented at the SPE Annual Technical Conference and Exhibition in New Orleans, Louisiana, 1982.
12. Standing M.B., 1947, "A Pressure-Volume-Temperature Correlation for Mixtures of California Oils and Gases", Drilling and Production Practice, 1947.
13. Oluseyi Harris, "Evaluation of equivalent circulating density of drilling fluids under high pressure-high temperature conditions", Master thesis, Norman Oklahoma 2004.
14. H. P. Lohne, J. E. Gravdal, E. W. Dvergsnes, G. Nygaard, E. H. Vefring, International Research Institute of Stavanger – IRIS," Automatic Calibration of Real-Time Computer Models in Intelligent Drilling Control Systems - Results From a North Sea Field Trial", IPTC 12707, International Petroleum Technology Conference, 3-5 December 2008, Kuala Lumpur, Malaysia.
15. Jan Einar Gravdal, Rolf J. Lorentzen, Kjell K. Fjelde, and Erlend H. Vefring ," Tuning of Computer Model Parameters in Managed-Pressure Drilling Applications Using an Unscented-Kalman-Filter Technique", SPE 97028-PA, International Research Institute of Stavanger, page 856-866, 2010.
16. Isabel C. Gil, Halliburton Energy Services; Sara Shayeg, "Comparison of Wellbore Hydraulics Models to Maximize Control of BHP and Minimize Risk of Formation Damage", SPE 81625-MS, IADC/SPE Underbalanced Technology Conference and Exhibition, 2003.

17. H. Rabia: / Oilwell drilling engineering : principles and practice / London : Graham & Trotman, 1992.
18. Roozbeh Ranjbar," Cuttings transport in inclined and horizontal wellbore", Master thesis, Stavanger University, 2010.
19. http://www.iris.no/Internet/energy.nsf/wvDocID/380F9DF24C646856C12578CD004485BE
20. http://www.iris.no/Internet/IntOpera.nsf/wvDocID/95695B7637AB6CC5C12572990049873 3
21. Eric Cayeux, Benoît Daireaux, Erik Wolden Dvergsnes, IRIS, Gunnstein Sælevik, Sekal," Early Symptom Detection Based on Real-Time Evaluation of Downhole Conditions: Principles and Results from several North Sea Drilling Operations", SPE 150422-MS, presented at SPE Intelligent Energy International, Utrecht, The Netherlands, March 2012.
22. Eric Cayeux, Benoit Daireaux, Erik W. Dvergsnes, IRIS, " DrillScene Technology Description" Report by IRIS, 2011
23. Egil Ronaes, Truls Fossdal, and Tore Stock, M-I SWACO," Real-Time Drilling Fluid Monitoring and Analysis - Adding to Integrated Drilling Operations", SPE 151459, presented at the IADC/SPE Drilling and Exhibition in San Diego, California, USA 2012.
24. Cayeux E., Daireaux B., Dvergsnes E., Sælevik G., Zidan M., 2012, "An Early Warning System for Identifying Drilling Problems: An Example From a Problematic Drill-Out Cement Operation in the North-Sea", paper SPE 150942 presented at the SPE Drilling Conference in San Diego, California, USA, 6-8 March, 2012.
25. F.P. Iversen, E. Cayeux, E.W. Dvergsnes, J.E. Gravdal, and E.H. Vefring, Intl. Research Inst. of Stavanger (IRIS); B. Mykletun, NOV; A. Torsvoll and S. Omdal, Statoil; and A. Merlo, Eni Agip SpA, "Monitoring and Control of Drilling Utilizing Continuously Updated Process Models", SPE 99207, presented at the IADC/SPE Drilling Conference, Miami, Florida 2006.